Chapter 5
Practical Aspects of Geostatistics in Hazardous, Toxic, and Radioactive Waste Site Investigations

5-1. General

a. In this chapter, several example applications are described. The applications have been developed using hydrologic, geologic, and contaminant data from established and well-studied hazardous waste sites. The real nature of the data permits discussion of some problems that can occur during HTRW site investigations that stem not only from natural field conditions, but also from typical problems that are associated with the types of data involved. In addition, the real nature of the example data provides an opportunity for comparison between kriging estimates and the real data. In accordance with the purpose and scope of this ETL, these comparisons will be brief and general. This ETL does not provide the comprehensive analysis of data that is addressed by other more elaborate studies.

b. The principal intent of the examples is to provide systematic descriptions for a few of the large number of possible types of applications that investigators may use during HTRW site investigations. The examples are not intended to provide guidance for comprehensive analysis of the included data. This ETL will, however, present some fundamental problems that can occur in geostatistical applications and, in some examples, indicate some possible alternatives.

c. With each example, a purpose will be established and a general environmental setting will be given. Most aspects of variogram construction and calibration will be briefly described and illustrated graphically and in tabular form. A comprehensive treatment of variogram construction has been presented in Chapter 4.

d. GEO-EAS software has been used whenever the example data did not need universal kriging; for those examples, STATPAC was used. As indicated in Chapter 3, both of these software packages run on the DOS platform (Table 3-1), which will probably be most convenient to readers. The results of kriging estimates are portrayed by gray-scale maps rather than by contours because of the objective nature of the gray-scale format. North is at the top of all maps presented in this ETL, although this orientation may represent some deviation from the real data.

5-2. Water-Level Examples

a. The following examples are for groundwater levels. The principal purpose of the examples is to expose the reader to a kriging exercise using groundwater levels and to indicate how, in a simple manner, kriging standard deviations may be useful to investigators interested in evaluating monitoring networks. The data come from a water-table setting in unconsolidated sediments where the local relief for the land surface is about 30 m. The data involved in this example are considered virtually free of actual measurement error.

b. The location of measured water levels is shown in Figure 5-1a and the basic univariate statistics for this data set are listed in Table 4-1; modifications to the measured data, in the form of addition and removal of measured values, are shown in Figures 5-1b and 5-1c. The techniques described in Chapter 4 were used to guide the following steps for variogram construction:

(1) A raw variogram analysis, along with basic hydrologic knowledge of water-level behavior, indicated that universal kriging would be needed for this analysis.

(2) To obtain a stable variogram of residuals, an iterative, generalized least-squares operation was initially used to remove prominent linear drift of the form $a + bu + cv$, observed in the measured water levels.

(3) After drift was removed, residuals were determined to be stationary and universal kriging with a linear drift was appropriate.

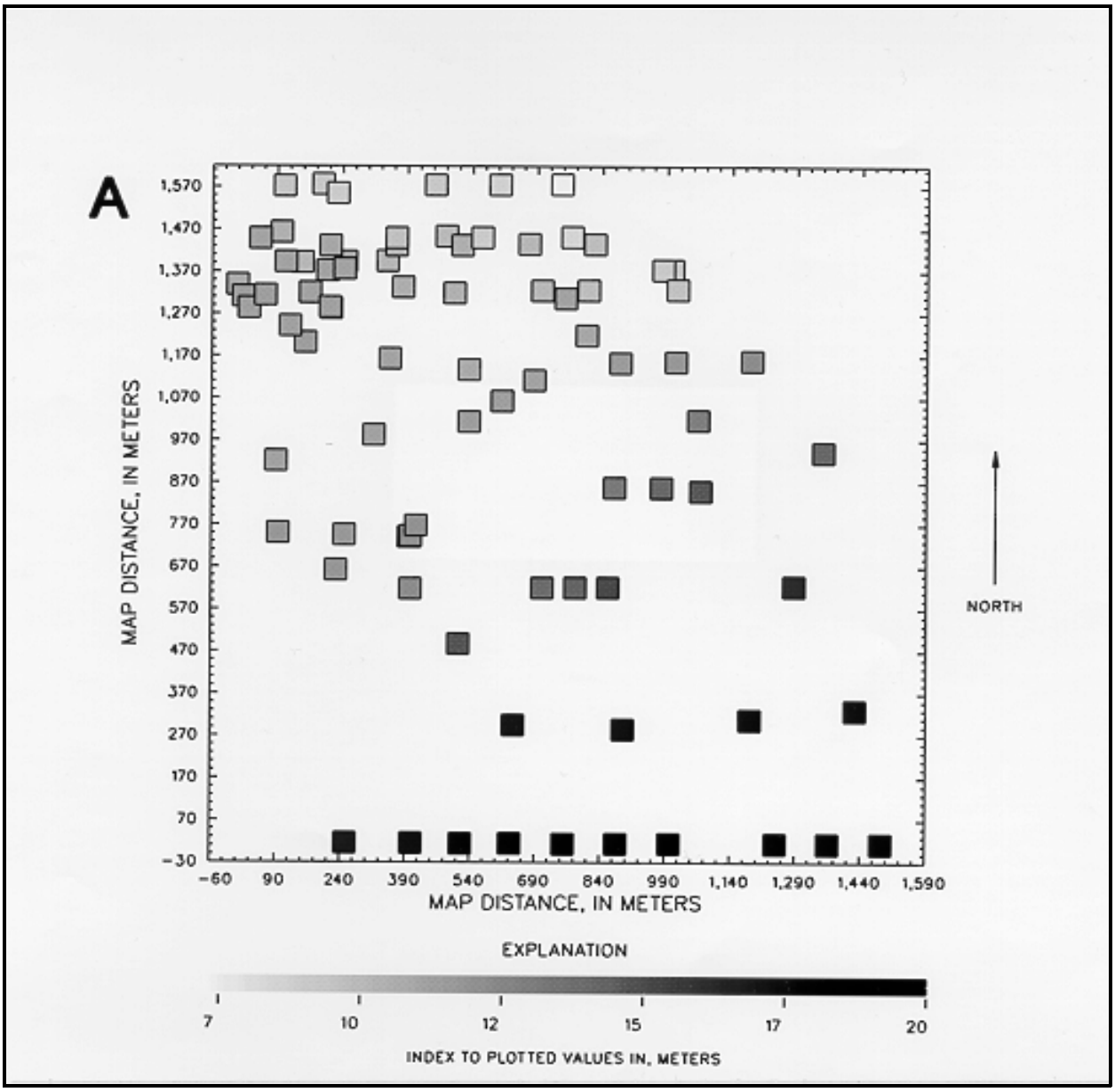

Figure 5-1. Measured data for water-level examples--A, original data; B, original data without dropped sites; C, original data with added sites (added sites indicated with +) (Sheet 1 of 3)

A Gaussian model was used to fit the stabilized variogram of residuals (Figure 5-2a), which has a nugget of 0.093 m^2, a sill of 2.69 m^2 and a range of 1,219 m (Table 5-1).

(5) Cross-validation was performed, and the results are shown in Figures 5-2b and 5-2c, and listed in Table 5-1. Cross-validation statistics conform to the criteria discussed in Chapter 4.

c. Linear drift is commonly observed in groundwater elevation data where there are no major anthropogenic activities, such as large groundwater withdrawals. With these

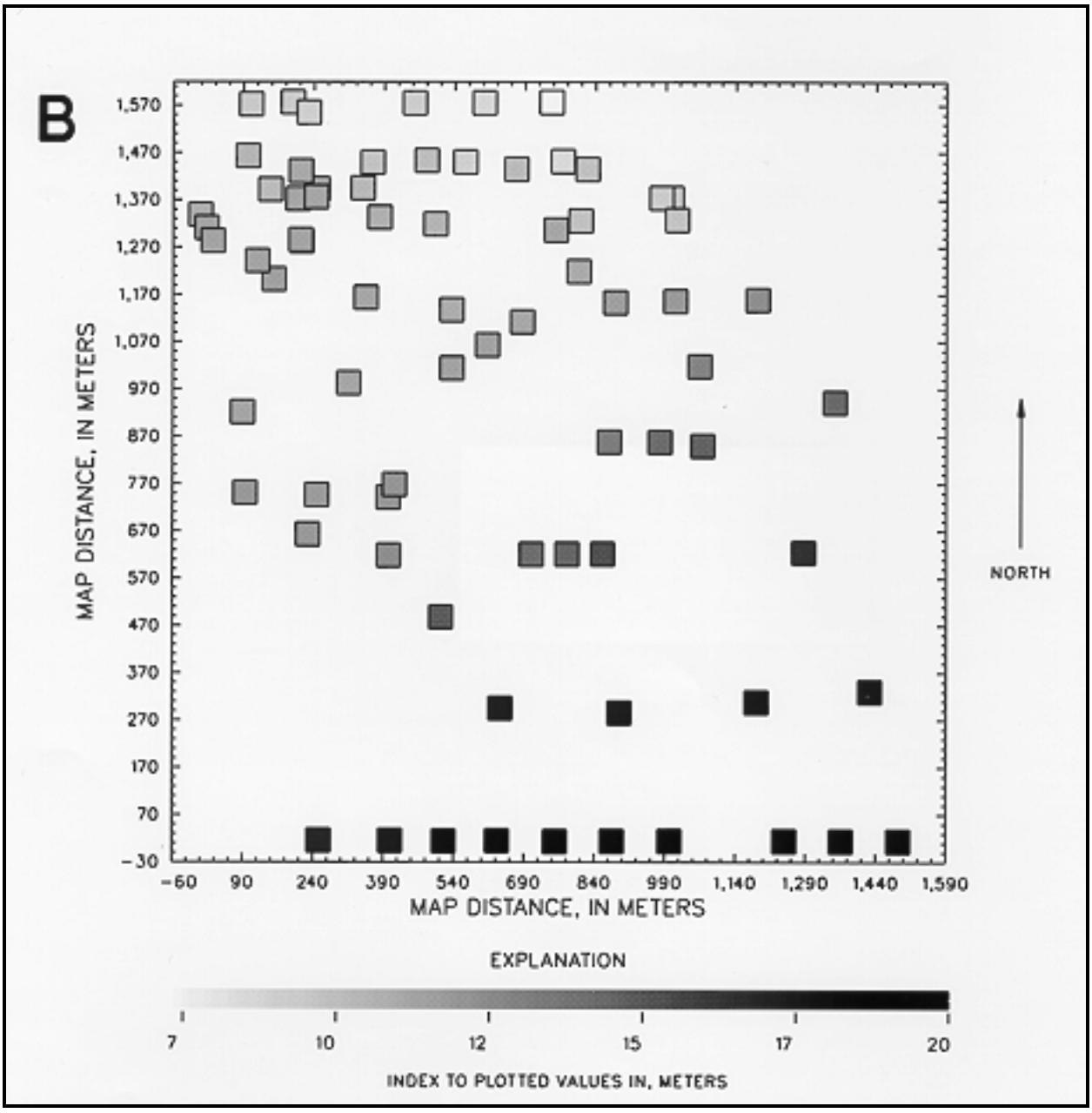

Figure 5-1. (Sheet 2 of 3)

circumstances there is usually a fairly uniform and general groundwater movement that is generally expressed in terms of direction. This uniform and general nature introduces a nonstationary element to the data that, in geostatistics, is referred to as drift. As indicated in Chapter 4, the presence of drift is indicated by a parabolic variogram shape. In this example, the initial variogram in the raw variogram analysis had a characteristic parabolic shape and a linear drift was identified. Once the drift was identified and characterized, universal kriging procedures were used.

d. A Gaussian model is usually appropriate for variograms with highly continuous variables such as groundwater-elevation data, and it is particularly appropriate in this example. The variogram (Figure 5-2a) at small lags beyond the nugget

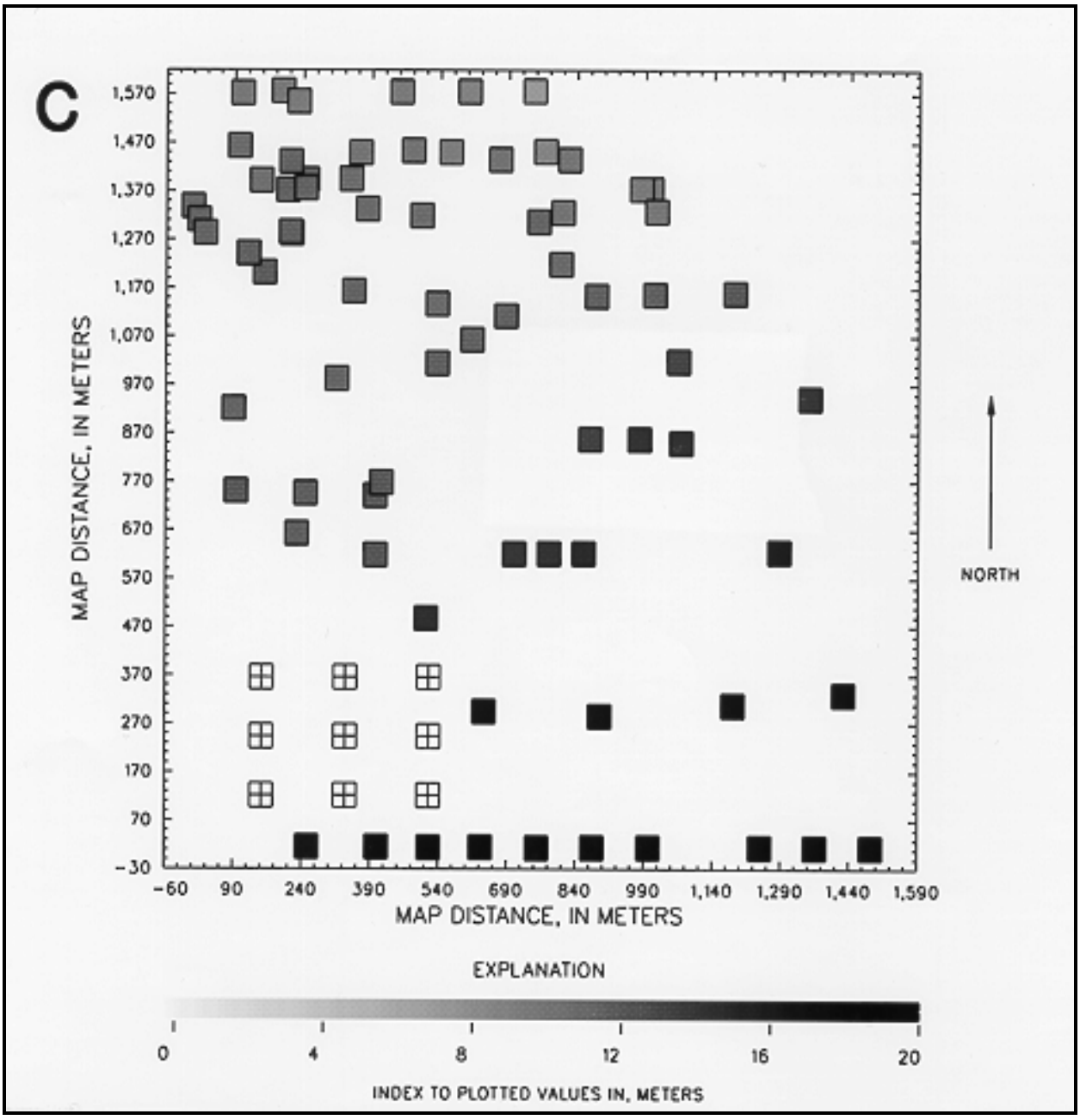

Figure 5-1. (Sheet 3 of 3)

has an upward concavity that cannot be fit with a linear, spherical, or exponential model. The observed shape was interpreted as a function of continuous small-scale variability. The Gaussian model fits the bowl shape of the small lag data (and other data to a lag of about 610 m) well, but it is not flexible enough to closely fit the points much beyond 610 m, indicating that kriging estimates should be computed using neighborhoods with a search radius less than 610 m. In Chapter 4, the initial part of the variogram was described as having the most effect on subsequent kriging estimates.

e. The established variogram then was used with the measured data to produce universal

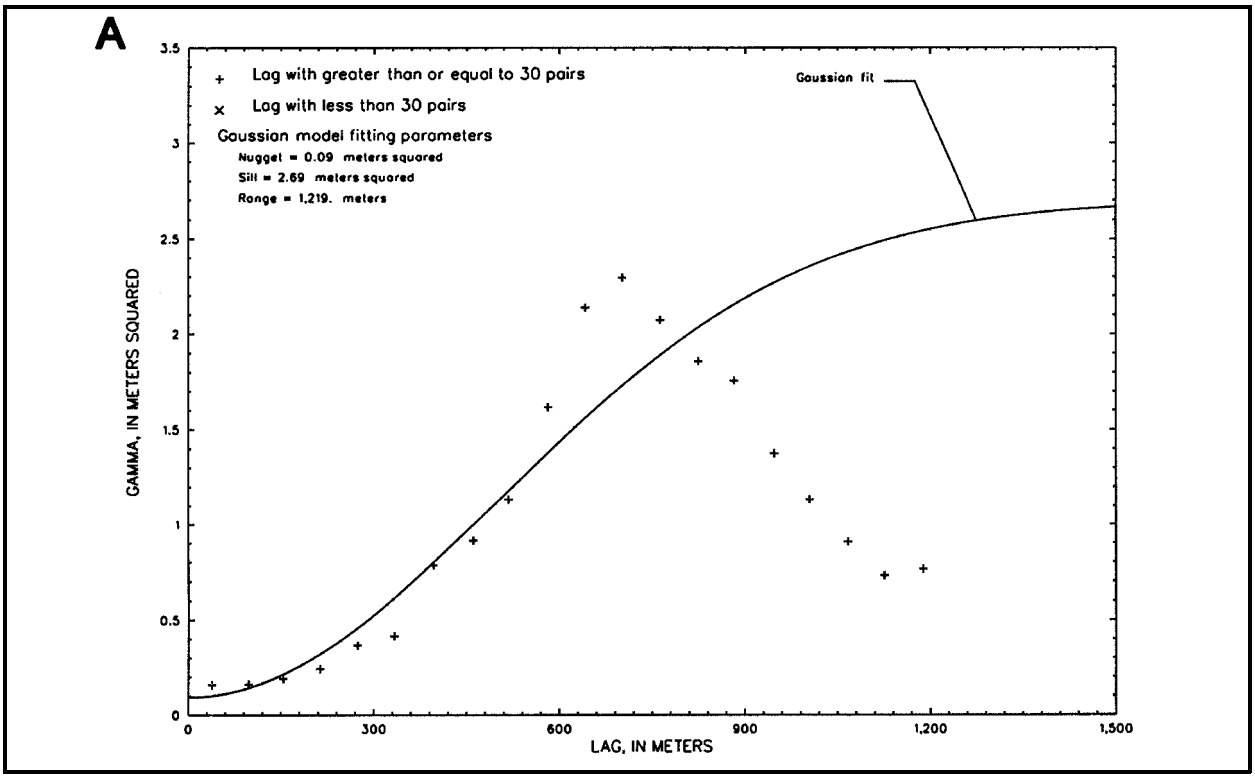

Figure 5-2. Variogram and variogram cross-validation plots for residuals in water-level example--A, theoretical variogram; B, cross-validation scatterplot; C, cross-validation probability plot (Sheet 1 of 3)

kriging estimates for all points in a 26-by-26 grid with a grid size of about 61-by-61 m. A gray-scale map of the kriging water levels is shown in Figure 5-3a and basic univariate kriging estimate statistics are listed in Table 5-2a (water level A). The kriging results a are a good representation of the results from other more elaborate studies.

f. Kriging standard deviations for the kriging estimates are shown in Figure 5-3b. The magnitude of kriging standard deviations can provide investigators with a direct indication of where the uncertainty associated with kriging estimates is relatively high or low. The areas of greatest uncertainty for the kriged water levels are in the upper right and lower left corners of the map, where standard deviations are as high as about 1.4 and 0.8. Not surprisingly, these areas are where the density of the measured data is relatively low. Throughout much of the remainder (about 70 percent) of the map, the kriging standard deviation is almost constant at about 0.35.

g. To use the kriging standard-deviation values in a more quantitative manner, the investigator needs to establish some assurance that the measured data and the reduced kriging errors are approximately normally distributed and also that the assumption of stationary residuals after drift removal is correct. If the investigator is confident about these assumptions, then the basic statistical principles involving confidence intervals can be applied. In this example, the standard deviation of about 0.35 throughout most of the map indicates that there is a 95-percent chance that the true value at a location where there is a kriging estimate will be within about 0.70 (twice the kriging standard deviation) of the kriging estimate.

h. As an example of evaluating network density and the accuracy of kriging estimates, two new maps were developed. To make the first map, a decrease in network density was effected by removing nine measured locations from the northwest part of the area (Figure 5-1b) where sampling

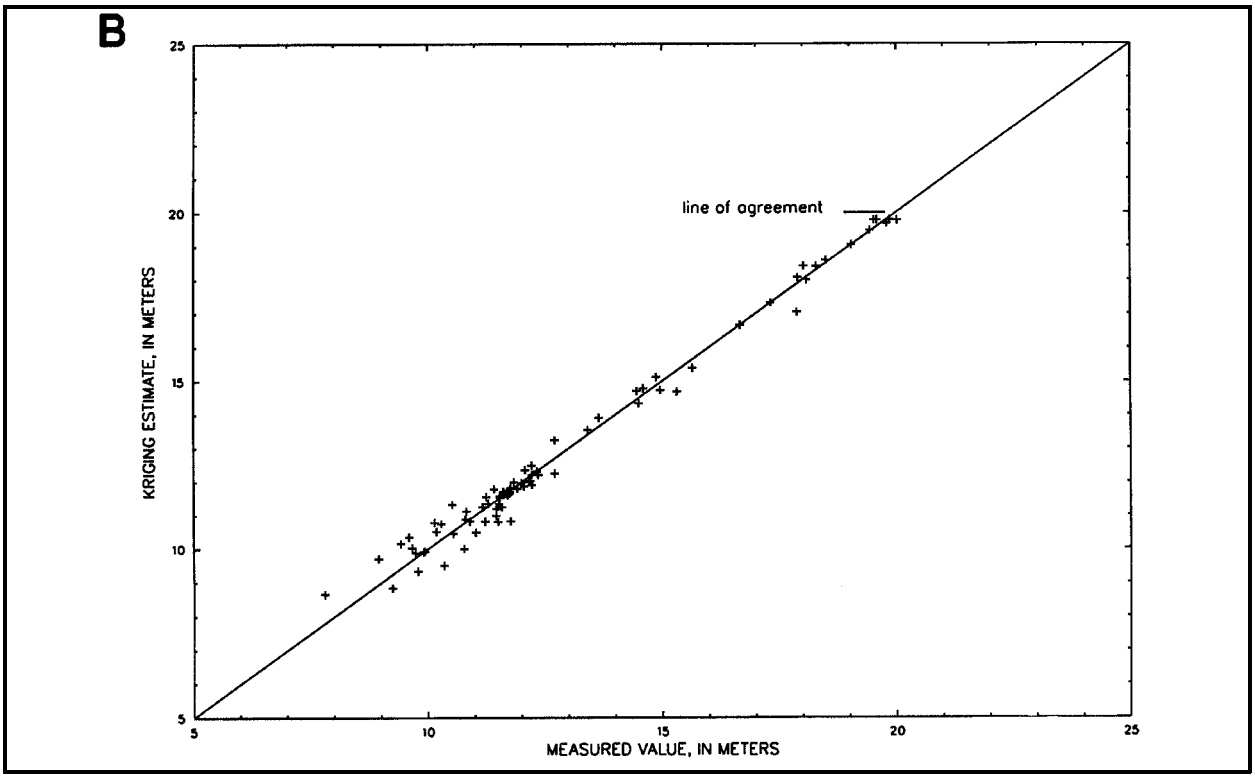

Figure 5-2. (Sheet 2 of 3)

density was high and kriging standard deviations were low. Kriging estimates were produced for the same grid and the basic univariate kriging estimate statistics are listed in Table 5-2 (water level B). The map shown in Figure 5-3c indicates that the ratio of the original kriging standard deviations and the kriging standard deviations with the nine measured locations removed is always very close to 1.00, which indicates that there is very little difference between the two sets of kriging standard deviations and that water levels are oversampled in the area where the nine measured locations were removed.

i. To produce the second map (Figure 5-1c) nine locations were added in the southwest corner where the sampling density was relatively low and the kriging standard deviation was relatively high. In section 2-4, Equation 2-47 indicates that the universal kriging variance depends on the variogram, the type of trend, and measurement locations; in this respect the kriging standard deviation does not depend on the values at measurement locations. Consequently, values of zero were used for the nine new measurement locations and only the resultant map of kriging standard deviations (Figure 5-3d) is of interest. The map shows that the kriging standard deviations in the lower left corner, which formerly had values of about 0.8, have been decreased by a factor of approximately 0.25, which indicates that the kriging estimates, based on the geometry of the network, are more reliable.

5-3. Bedrock-Elevation Examples

a. The following examples are for bedrock elevations. The principal purposes of the examples are to familiarize the reader with a kriging exercise using bedrock elevations and to describe block kriging. The data come from an area where bedrock consists of a series of intercalated terrestrial deposits that have been weathered somewhat and then covered with alluvium. The opportunity for measurement error in these types of data is

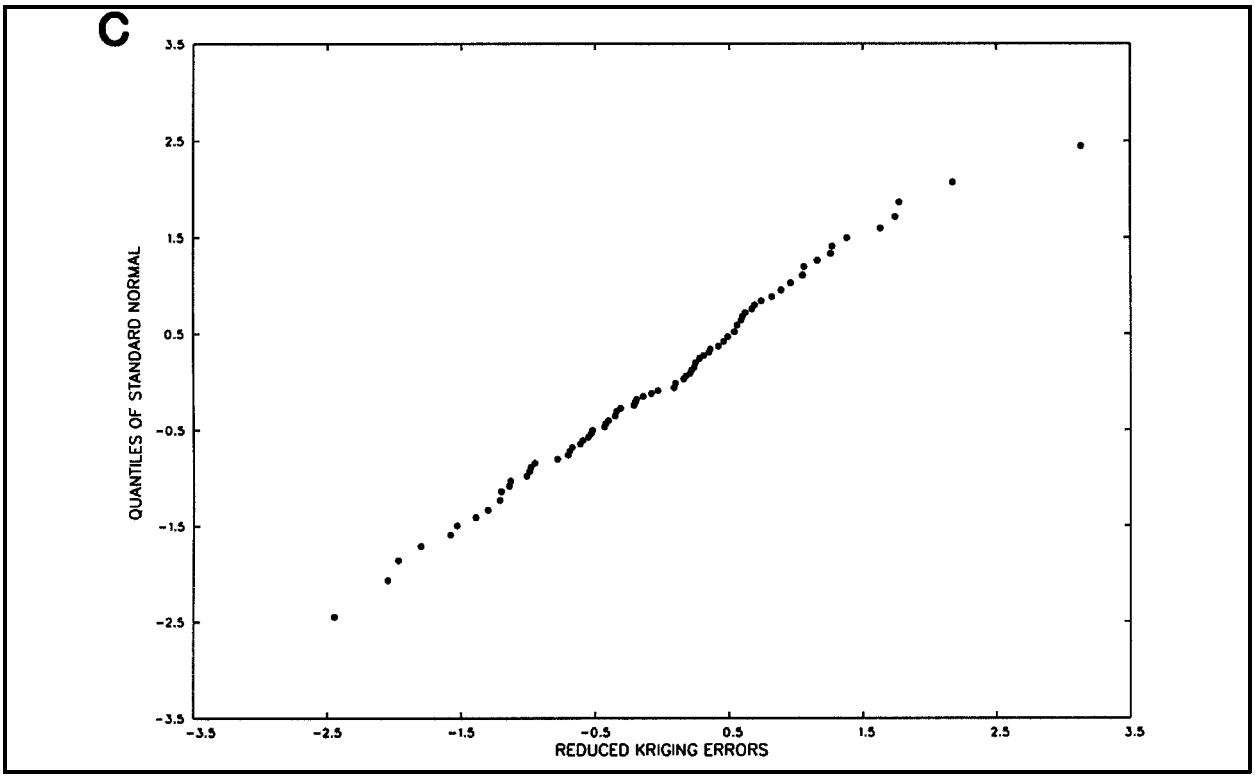

Figure 5-2. (Sheet 3 of 3)

inevitable because the determination of just where bedrock begins is complicated and subjective.

b. The set of measured locations, set A, is shown in Figure 5-4a and the basic univariate statistics are listed in Table 4-1 (bedrock A); modifications to the measured data, in the form of removal of sites is shown in Figure 5-4b. The techniques described in section 4-1 were used to guide the following steps for variogram construction:

(1) The raw variogram indicated a stationary spatial mean. The data were assumed to be suitable for ordinary kriging.

(2) An isotropic Gaussian model was used to fit the variogram which had a nugget of 0.650 m^2, a sill of 12.54 m^2, and a range of 914 m (Table 5-1, bedrock A).

(3) Cross-validation was performed, and the results, (Table 5-1, bedrock A), were not acceptable.

c. The cross-validation exercise produced a reduced-root-mean-squared error of 2.146 [Table 5-1 (bedrock A)] which indicates, as described in Chapter 4, that the kriging variance is underestimated to an unsatisfactory degree. Further attempts to fit the Gaussian model to the sample variogram points produced better cross-validation statistics; however, the Gaussian curve began to depart substantially from the sample variogram points at the lower lag sample points. As a result, the distribution of the residuals was explored, and the eastern, and especially northeastern, parts were determined to contain problematic data values that rendered the distribution nonhomogeneous. The nonhomogeneous nature is related to an incised channel present on the

Table 5-1
Variogram Characteristics and Cross-Validation Statistics[1]

	Variogram Characteristics						Cross-Validation Statistics		
Example Identifier	Transformation	Direction/ tolerance	Model	Nugget (Base units squared)	Sill (Base units squared)	Range (Base units)	Average Kriging Error (Base units)	Kriging Root-Mean-Squared Error (Base Units)	Reduced Root-Mean-Squared Error (dimensionless)
Water levels	Drift	0/NA	Gaussian	1.00	29.00	4,000.00	-0.002	1.20	1.083
Bedrock A	None	0/NA	Gaussian	7.00	135.00	3,000.00	0.146	8.30	2.146
Bedrock B	None	0/NA	Gaussian	8.00	90.00	2,400.00	-0.034	4.39	1.192
Water Quality A	Natural log	150/45	Exponential	1.00	3.20	4,250.00	0.105	1.54	0.938
Water Quality A	Natural log	240/45	Exponential	1.00	3.20	750.00	0.105	1.54	0.938
Water Quality B	Indicator	150/45	Spherical	0.05	0.25	2,000.00	NA	NA	NA
Water Quality B	Indicator	240/45	Spherical	0.05	0.25	700.00	NA	NA	NA

[1]NA= not applicable; base unit for water levels and bedrock is feet, base unit for water quality A is log concentration, concentration in micrograms per liter, base unit for water quality B is indicator units.

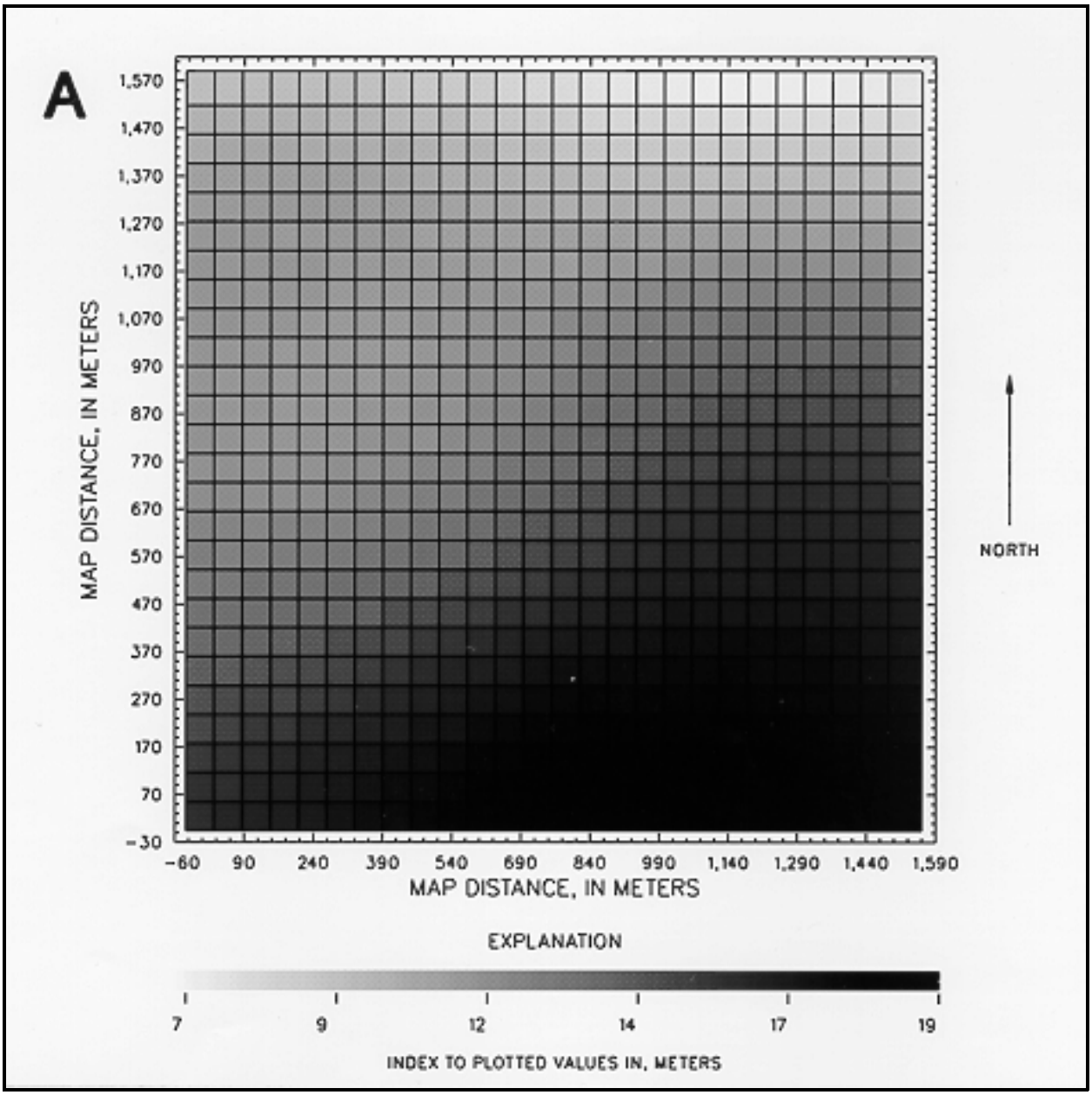

Figure 5-3. Kriging results for water-level examples--A, kriging estimates for original data; B, kriging standard deviations for original data; C, ratio (original data to original with dropped sites) of kringing standard deviations; D, kriging standard deviations for original data with added sites (Sheet 1 of 4)

bedrock surface. At this juncture, the measured data were restricted to exclude the outlying measurements. Before this decision was made, two alternative methods for dealing with the outlying values were considered and deemed beyond the scope of this effort. However, a brief discussion of the situation is appropriate.

d. The first alternative considered was to fit a contrived and nongradual surface to the measured data and remove the outlier effect. A splined surface could be capable of producing the desired result. The decision whether or not to pursue such a remedy becomes somewhat philosophical. In a relatively simple example, as in this bedrock

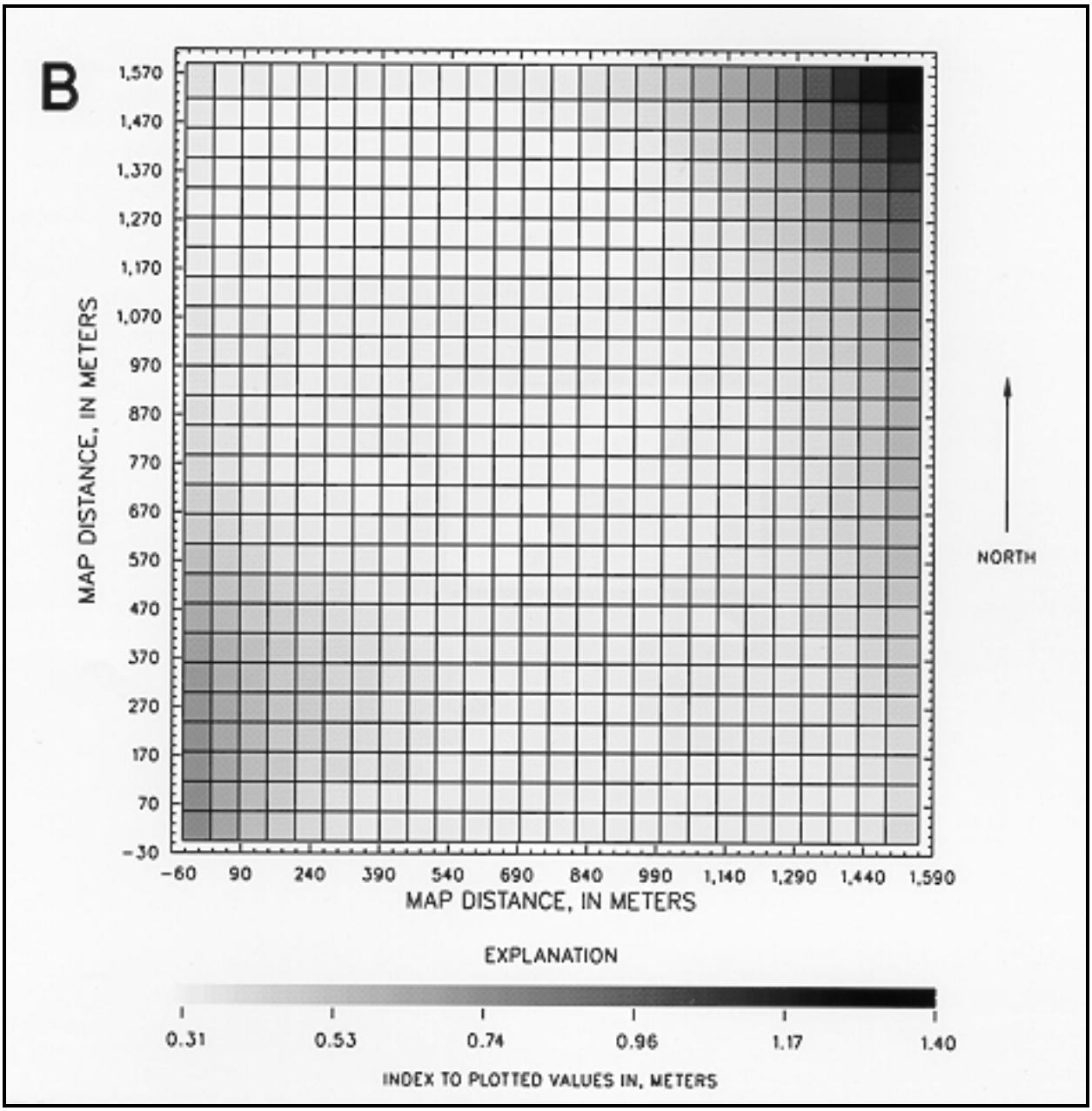

Figure 5-3. (Sheet 2 of 4)

example, such a remedy may be entirely appropriate; however, some investigators may support the idea that the situation is actually dealing with two unique and homogeneous domains. Therefore, the second alternative considered, distributing the kriging process so that each homogeneous domain is addressed independently, becomes more attractive. In more complicated applications where a large number of domains are present, a distributed approach may be necessary to avoid an undue amount of compromise.

e. The restriction of measured data, set B, is shown in Figure 5-4b and the basic univariate statistics are listed in Table 4-1 (bedrock B). The restriction exercise resulted in removing 17 measured locations and in the truncation of the northeastern part of the area so that the area became

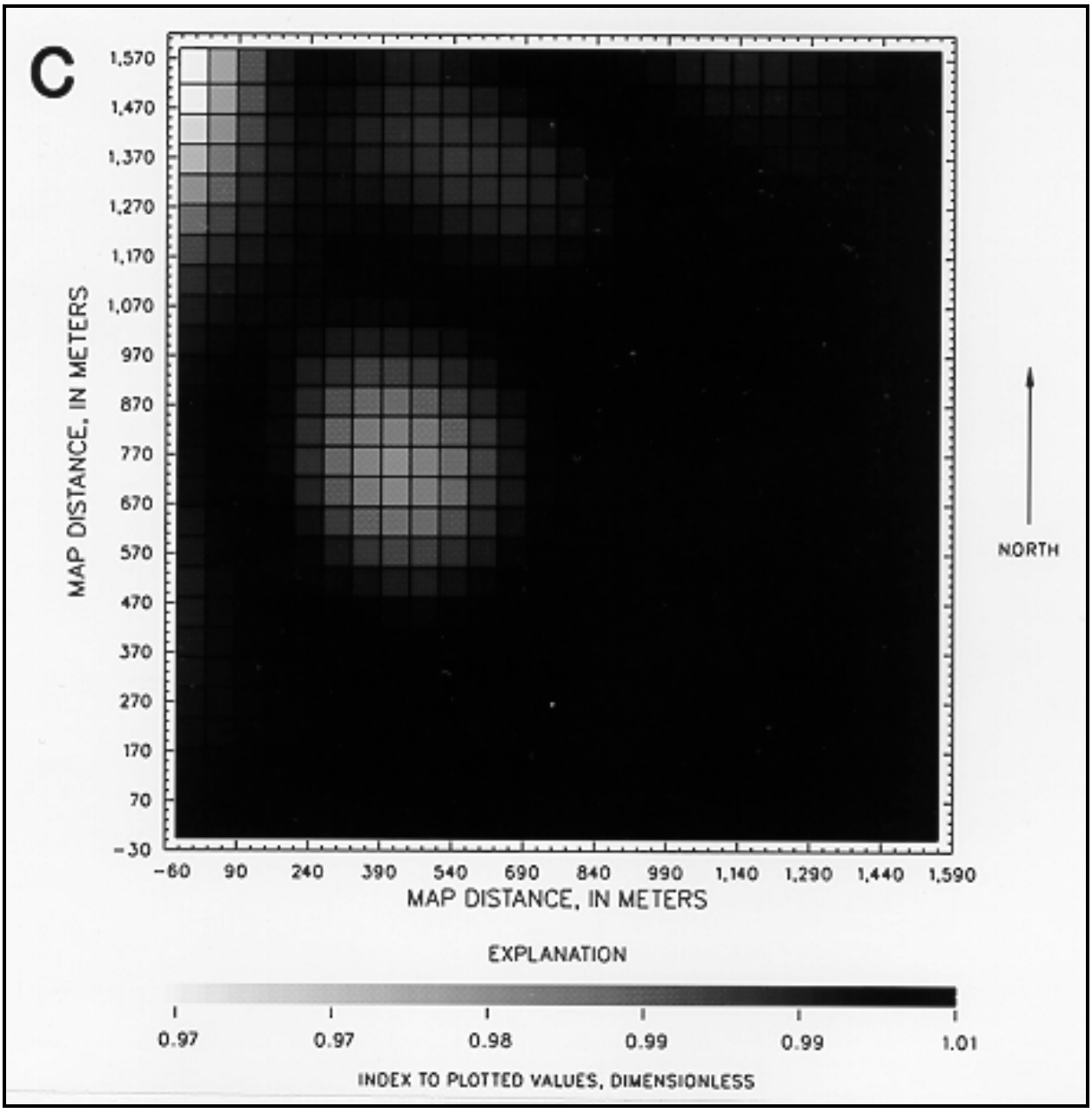

Figure 5-3. (Sheet 3 of 4)

polygonal rather than rectangular. Again, the techniques described in Chapter 4 were used to guide the following steps for variogram construction:

(1) A Gaussian model was used to fit the variogram which had a nugget of 0.650 m^2, a sill of 8.36 m^2, and a range of 732 m. The variogram indicated a stationary spatial mean.

(2) Initial cross-validation was performed, and the nugget was changed from 0.650 m^2 to 0.743 m^2 to improve cross-validation statistics. The final variogram is shown in Figure 5-5a and characteristics are listed in Table 5-1.

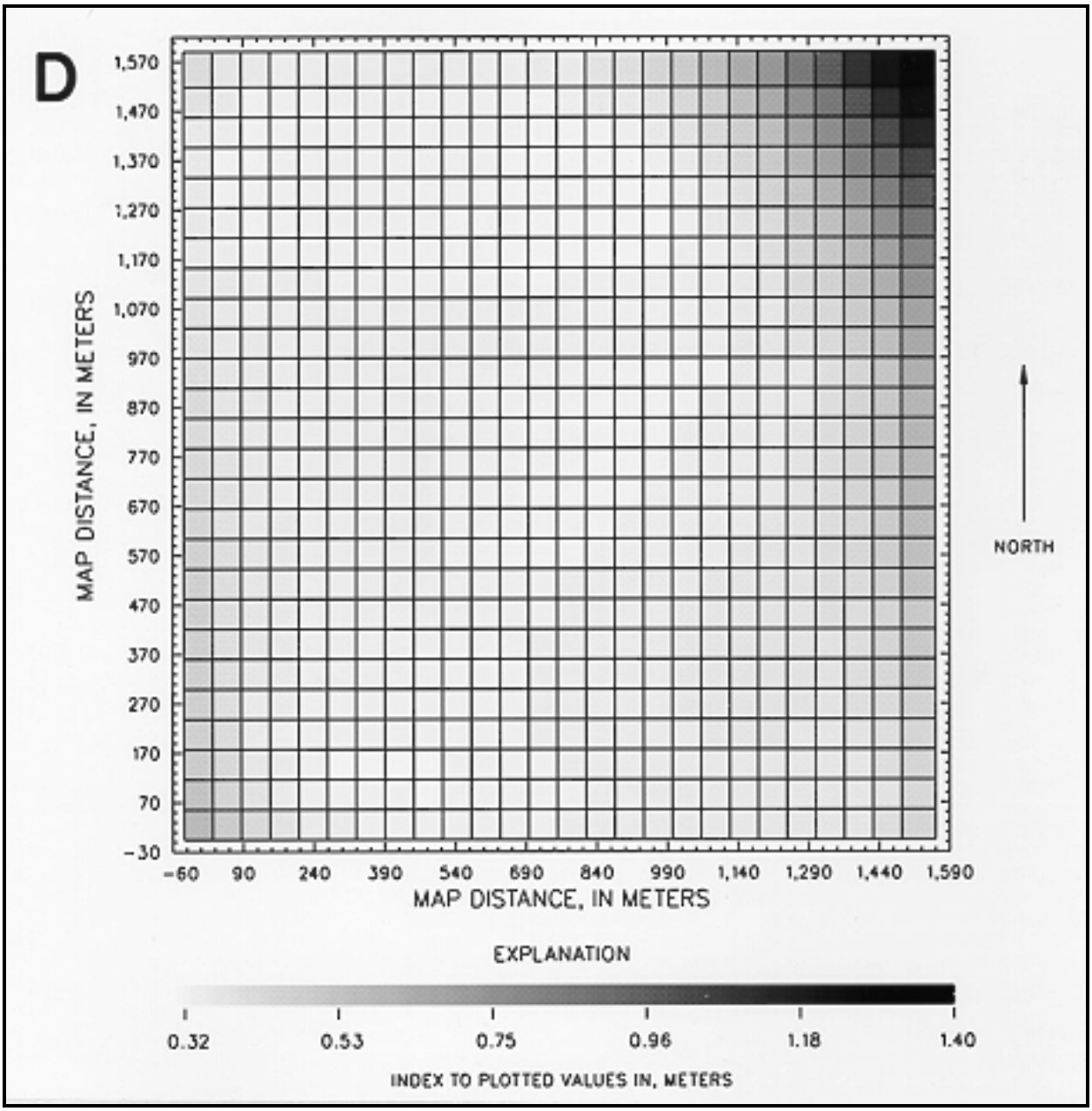

Figure 5-3. (Sheet 4 of 4)

(3) Final cross-validation was performed, and the results, shown on Figures 5-5b and 5-5c and listed in Table 5-1 (bedrock B), were acceptable.

f. The large difference between the sill defined for the initial data set and the sill for the restricted data set (12.54 m^2 and 8.36 m^2) supports the hypothesis that the original data set is actually two different domains. The final variogram then was used, along with the measured data, to produce ordinary kriging estimates for all points in a 52-by-52 grid with a spacing of about 30-by-30 m, which is truncated along the northeastern border because of the restriction operation. For the kriging procedure, a search radius of about 914 m witha maximum of 16 and minimum of 8 surrounding locations was specified. Gray-scale maps of the kriging estimates and kriging standard

Table 5-2
Univariate Statistics for Gridded Kriging Estimates in Example Applications[1]

Example Identifier	Transformation	Minimum (Base units)	Maximum (Base units)	Mean (Base units)	Median base units)	Standard deviation (base units)	Skewness (dimensionless)
Water level A	Drift	24.34	65.00	45.86	44.46	10.15	0.11
Water level B	Drift	24.59	65.00	45.84	44.45	10.14	0.11
Bedrock B	None	26.13	64.88	41.45	39.78	7.71	0.82
Bedrock C	None	26.72	64.39	41.50	39.69	7.63	0.82
Water quality A	Natural log	2.92	7.07	5.17	5.03	0.72	-0.06

[1]Base units for water level A and B and bedrock B and C is feet; base unit for water quality A is log concentration, concentration in micrograms per liter.

deviations are shown in Figures 5-6a and 5-6b, respectively, and the univariate kriging estimate statistics are listed in Table 5-2 (bedrock B). The kriging results indicate channel-like features in the bedrock surface, as well as a prominent bedrock high at the south border of the area; the results are a good representation of the results from other more elaborate studies.

g. For an example of block kriging, an investigative goal of establishing block values of bedrock elevation for a finite-difference groundwater model grid having about 120- by 120-m cells was assumed. The same variogram and search criteria were used to estimate block values for a 13-by-13 grid with about 120- by 120-m spacing; a 4-by-4 block was specified. Each kriging value shown in Figure 5-6c is interpreted as an estimate of the average value of bedrock elevation over the about 120- by 120-m block. The standard deviation for the block estimates is less than the standard deviation for the point estimates (Table 5-2). Gray-scale maps of the kriging estimates and the kriging standard deviations are shown in Figures 5-6c and 5-6d, and the univariate kriging estimate statistics are listed in Table 5-2 (bedrock C).

5-4. Water-Quality Examples

a. The following examples are for water-quality information consisting of concentrations determined for a contaminant. The principal purposes of the examples are to familiarize the reader with a kriging exercise using water-quality information and to illustrate indicator kriging. The examples also will familiarize the reader with data that are strongly anisotropic and need transformation. The data come from a water-table aquifer developed in alluvial sediments where the depth to water was less than about 23 m. Several analytical laboratories were involved in measuring the concentration of the contaminant in the water-quality examples. Each of the analytical laboratories was required to follow rather comprehensive guidelines that specified tests of instrument performance before sample determinations were made, as well as measurement of extraction efficiencies. Because of these performance guidelines, the opportunity for errors due to instrument error was considered to be either known or relatively low. In addition to using performance guidelines, field quality-assurance samples were also collected. These samples can be used to evaluate other types of possible errors, such as cross-contamination and representativeness of the sample. Duplicate samples for the contaminant in the water-quality examples indicate as much as 15 percent variability in reported results. This variability is not entirely unusual and is most likely related to the integrity of the analytical method or the method in which the sample media was aggregated during sample collection.

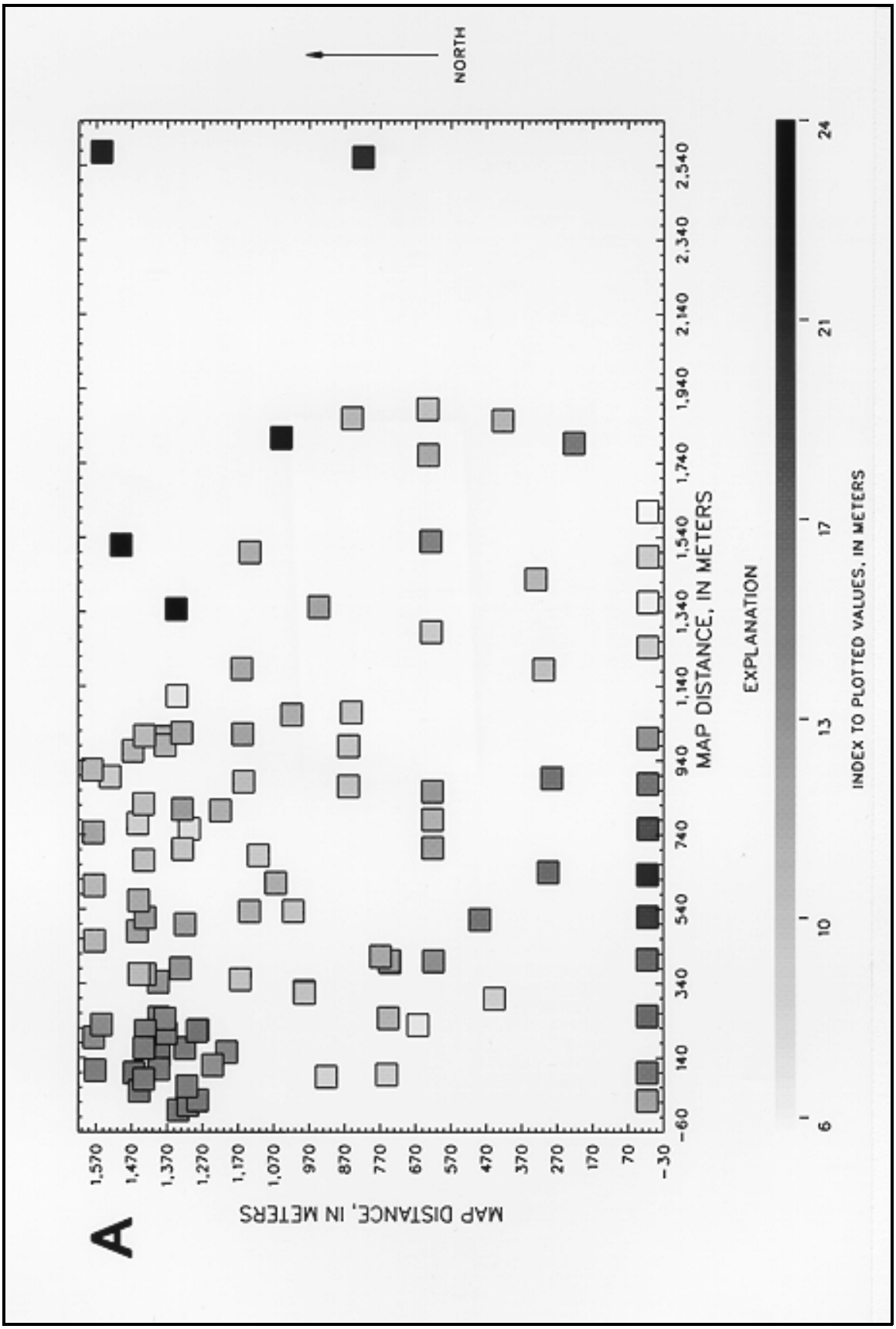

Figure 5-4. Measured data for bedrock-elevation examples--A, original data and B, restricted data (Continued)

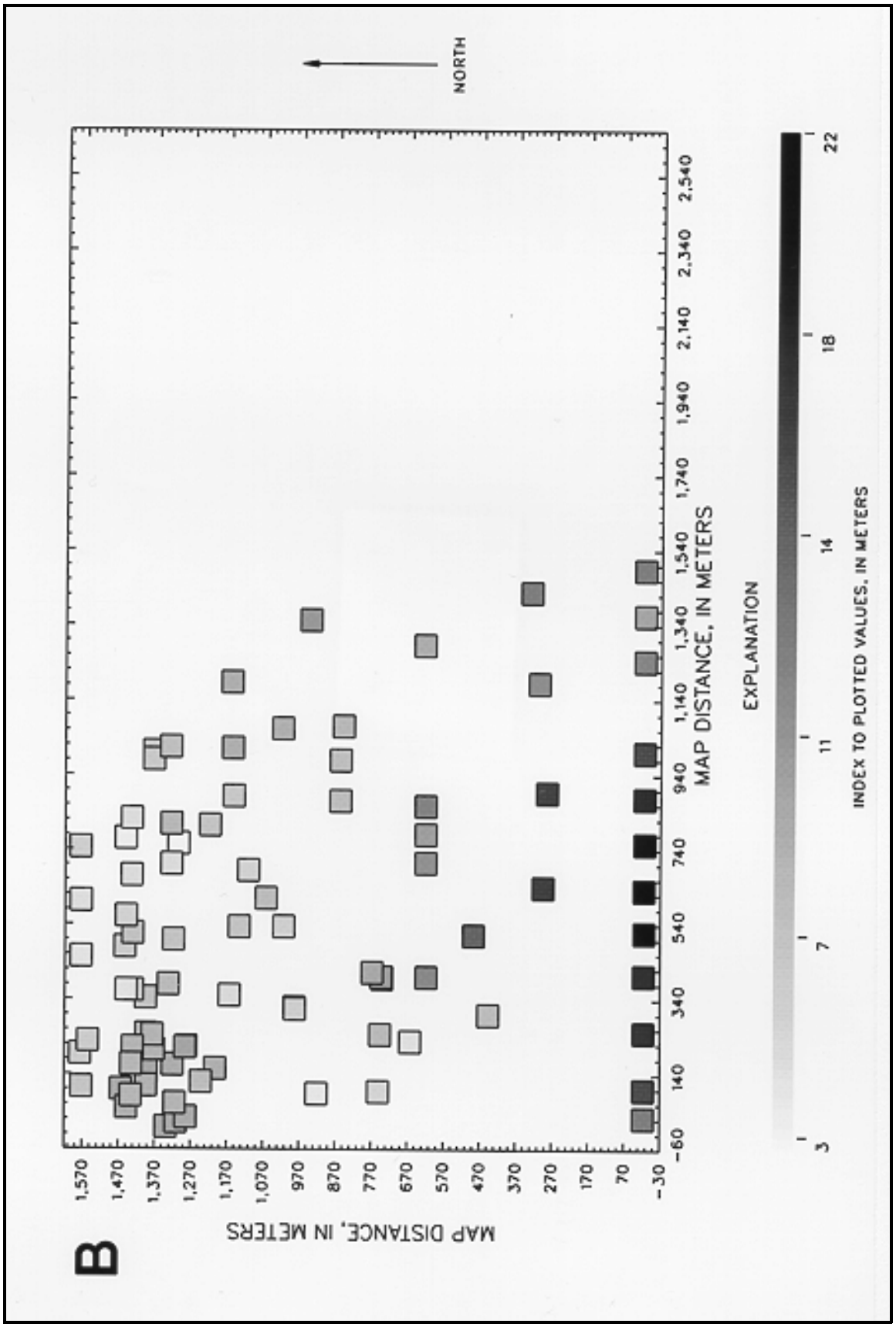

Figure 5-4. (Concluded)

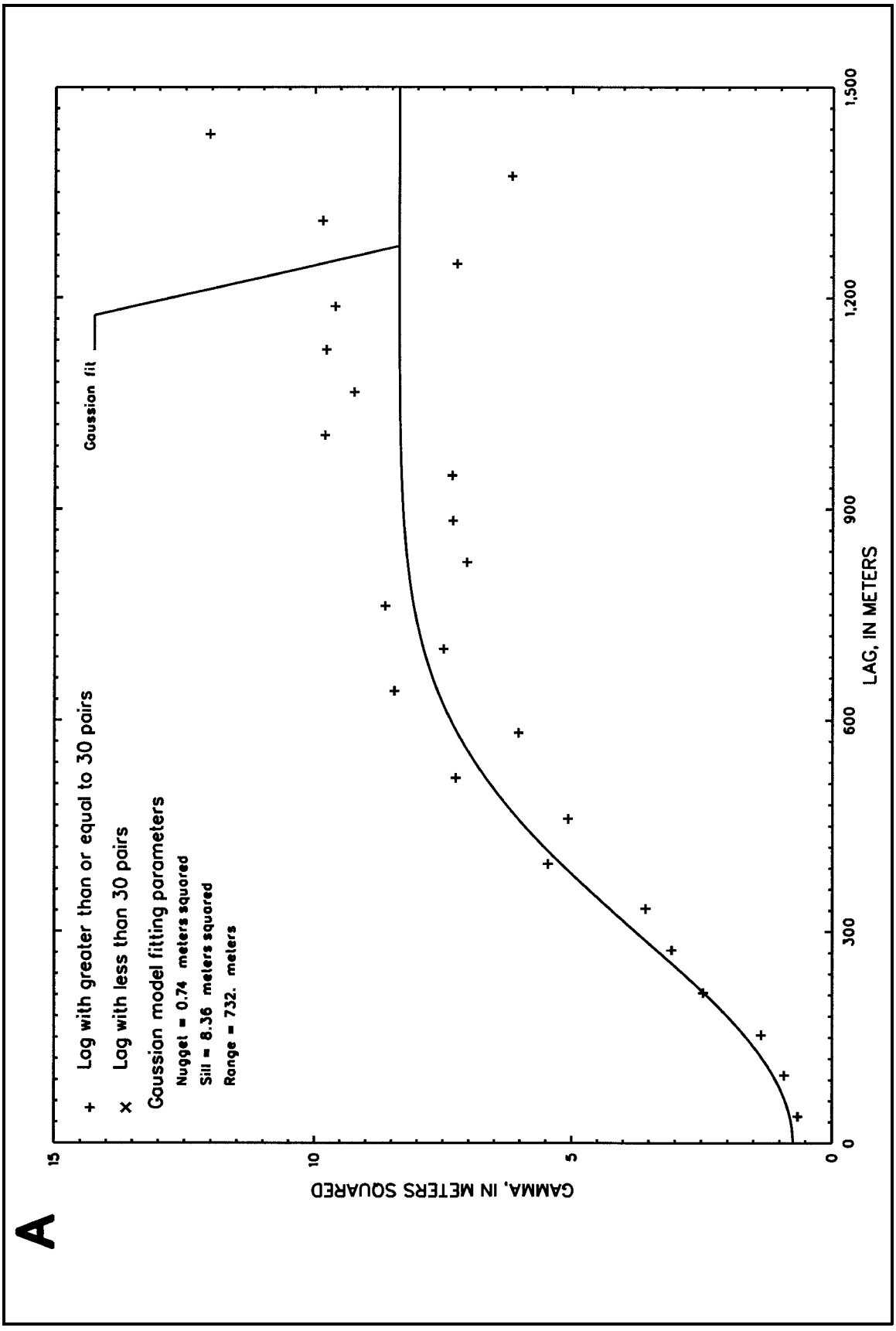

Figure 5-5. Variogram and variogram cross-validation plots for bedrock-elevation example--A, theoretical variogram; B, cross-validation scatterplot; C, cross-validation probability plot (Sheet 1 of 3)

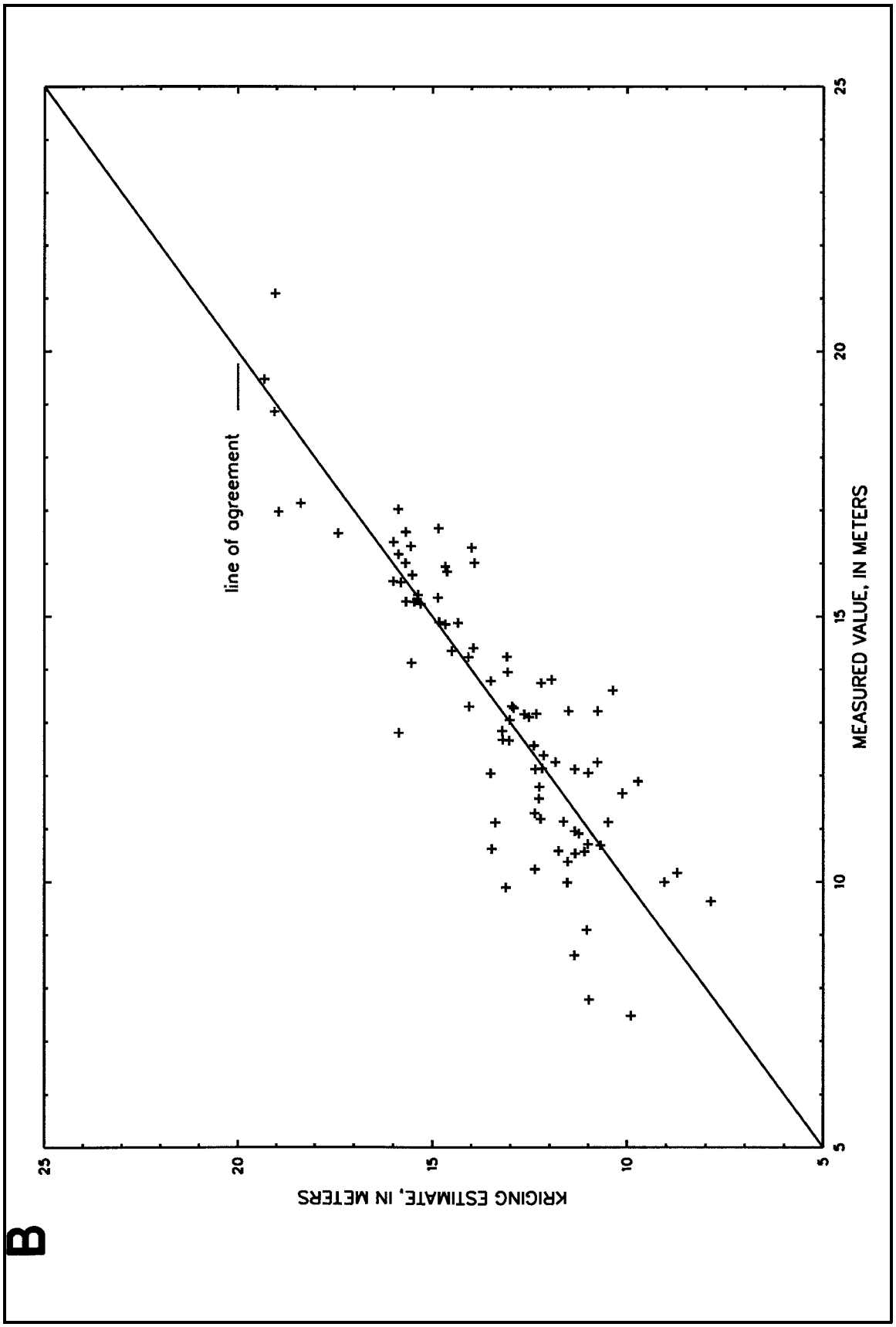

Figure 5-5. (Sheet 2 of 3)

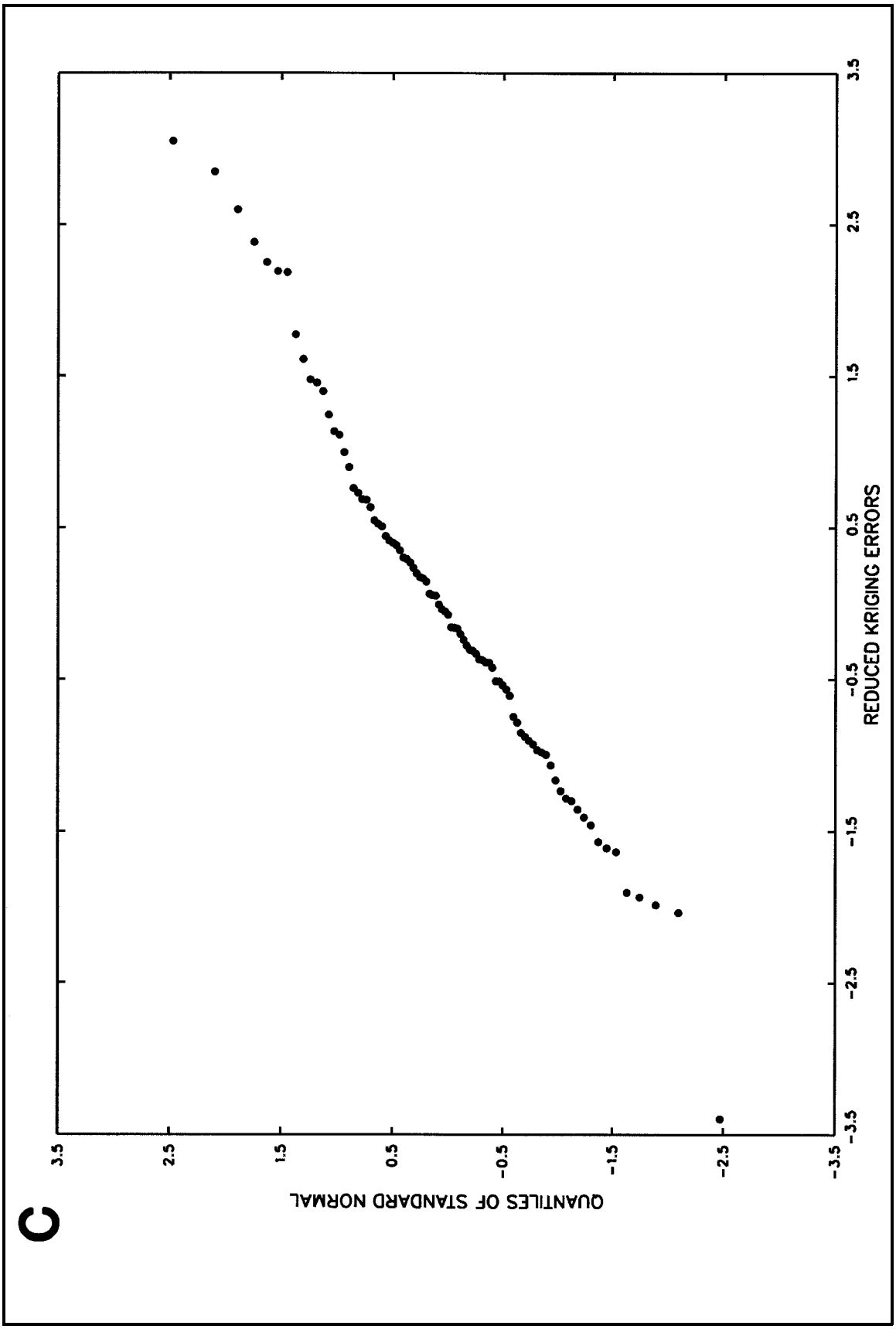

Figure 5-5. (Sheet 3 of 3)

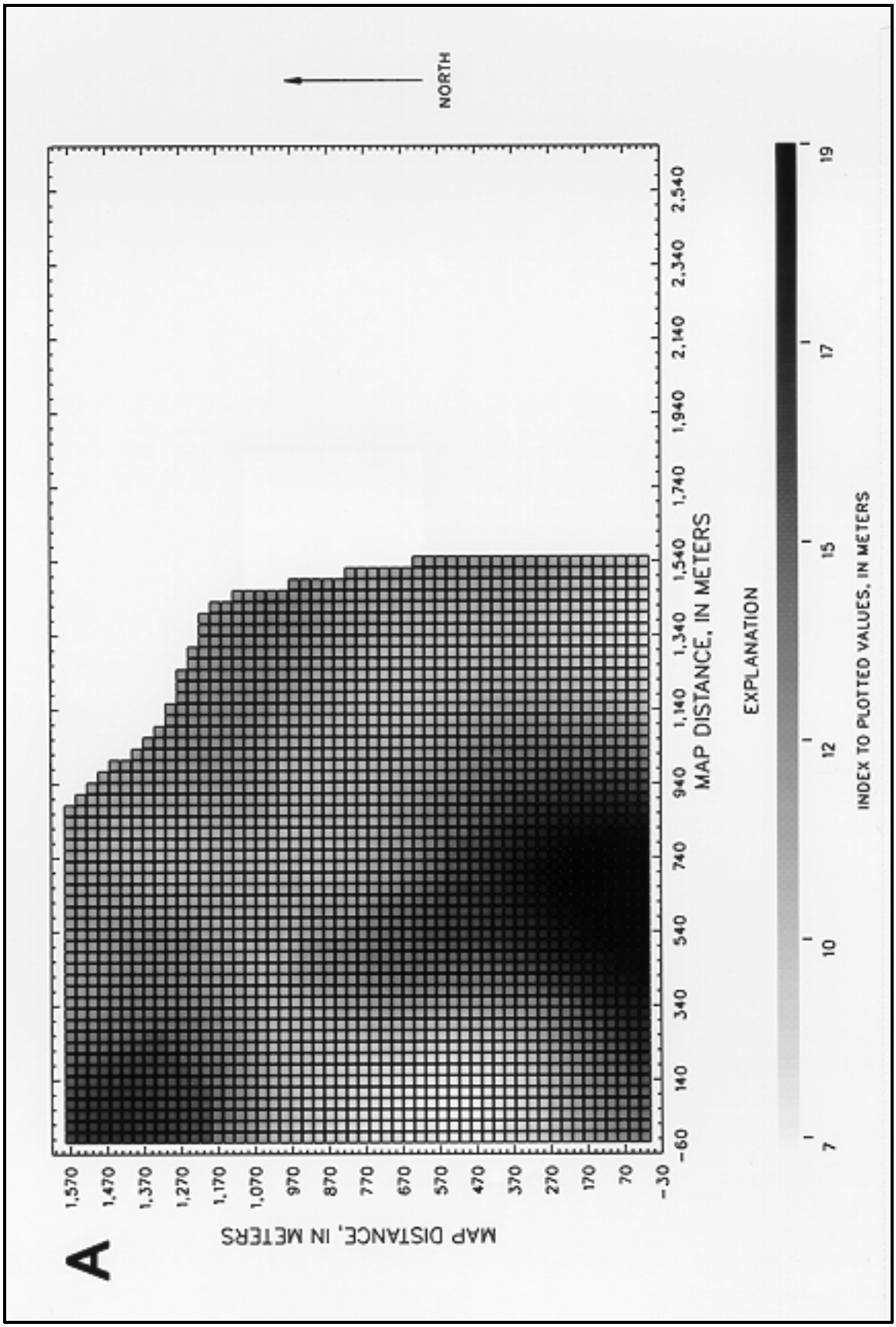

Figure 5-6. Kriging results for bedrock-elevation examples--A, kriging estimates; B, kriging standard deviations; C, block kriging results; D, block kriging standard deviations (Sheet 1 of 4)

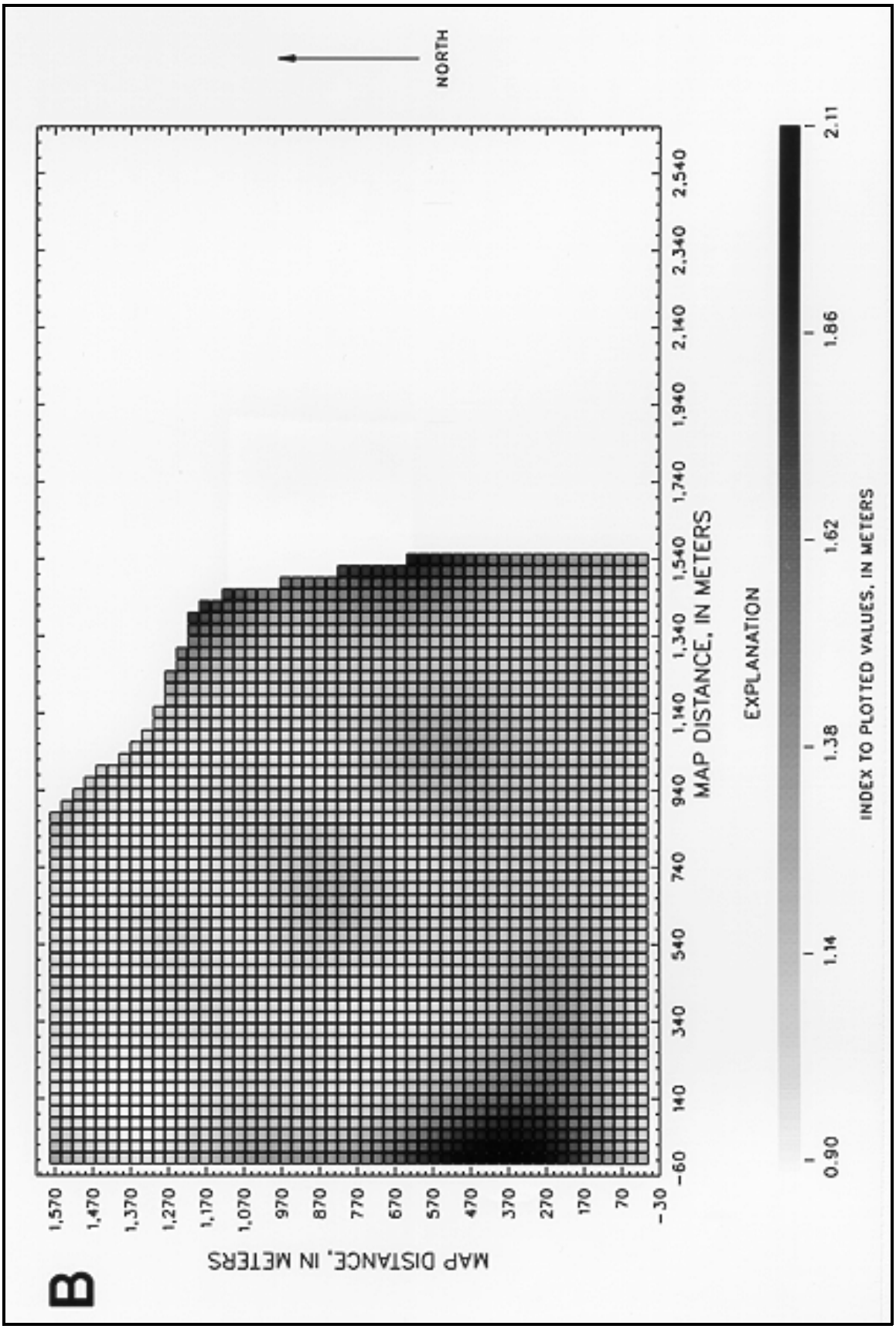

Figure 5-6. (Sheet 2 of 4)

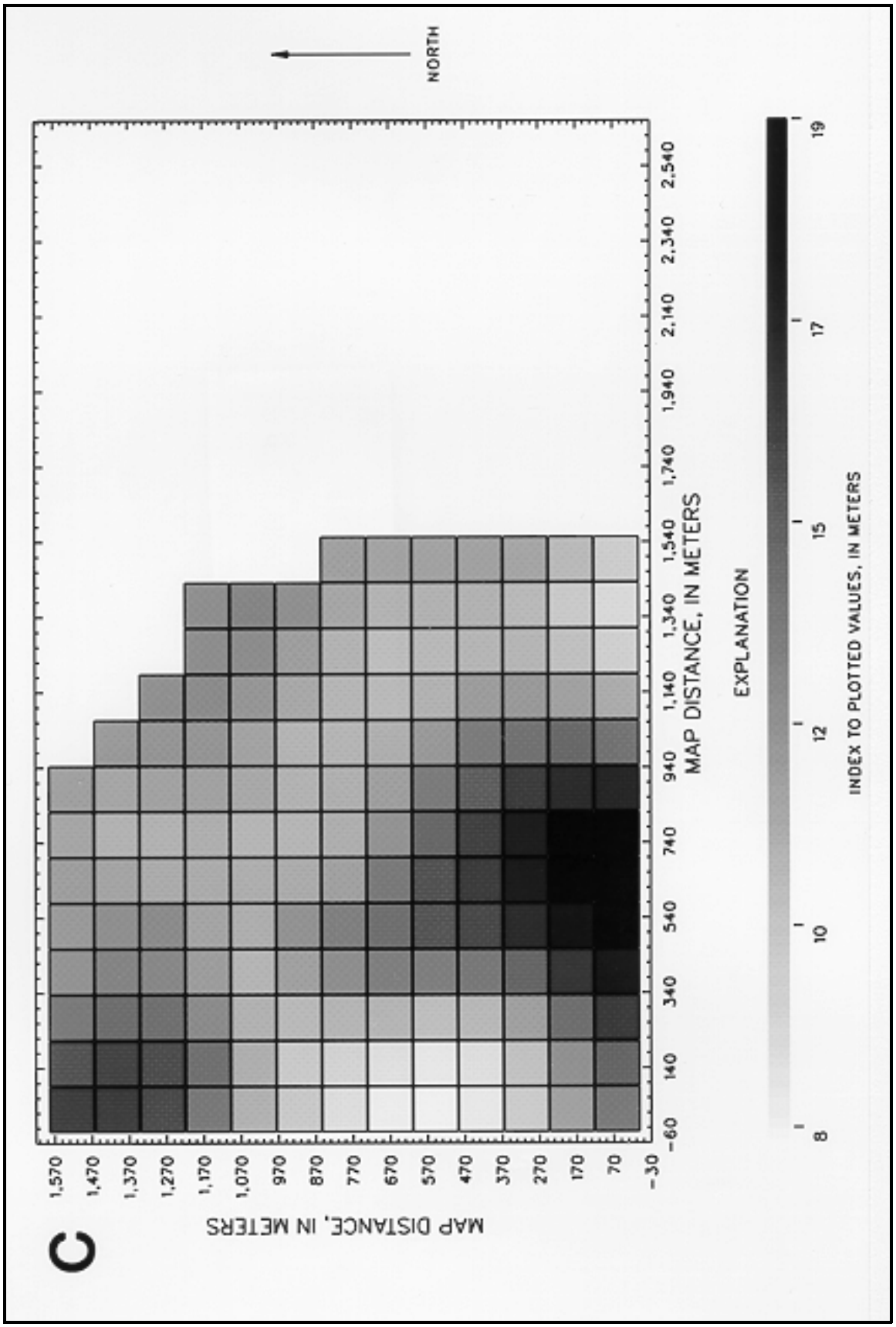

Figure 5-6. (Sheet 3 of 4)

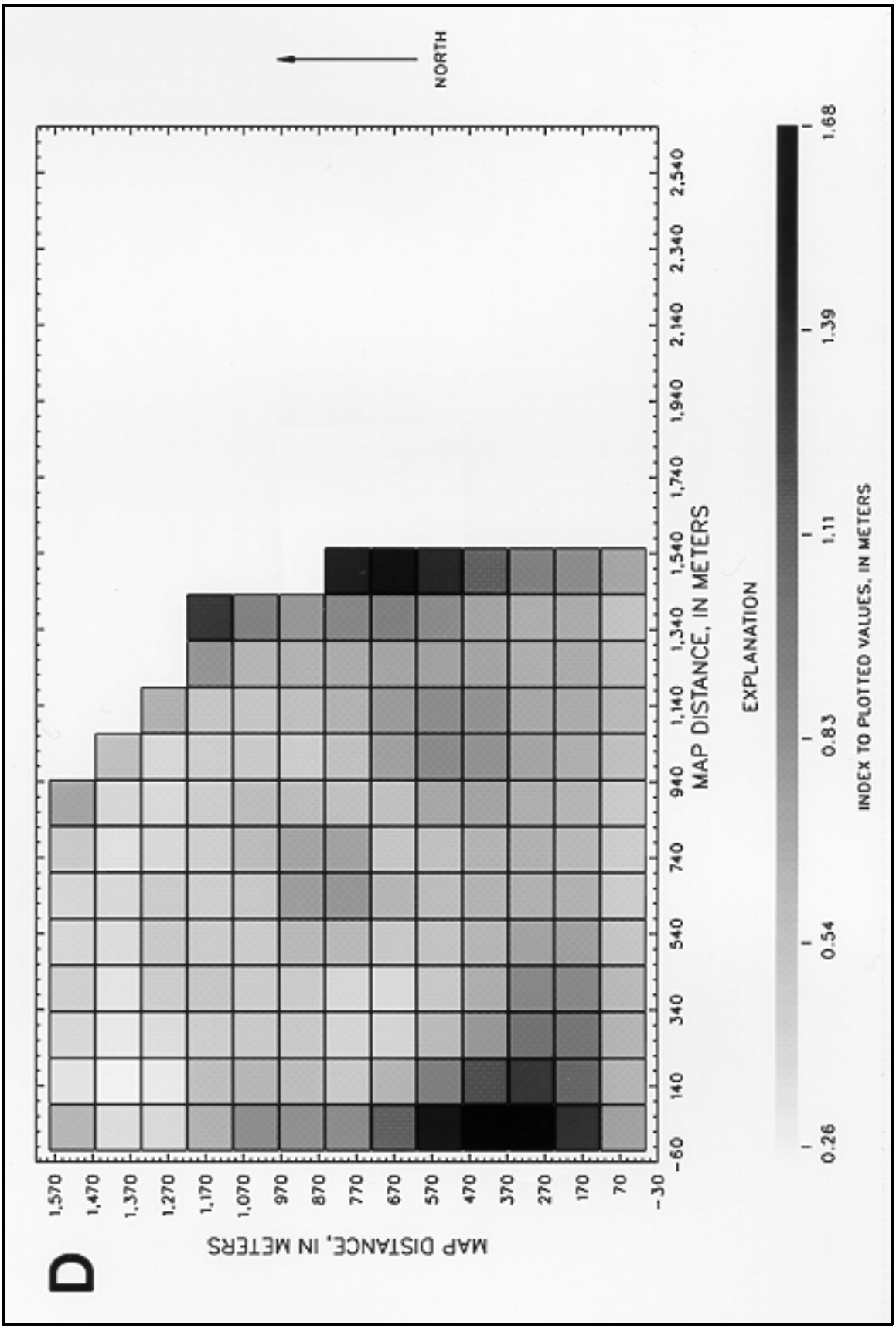

Figure 5-6. (Sheet 4 of 4)

b. Measured locations are shown in Figure 5-7 and the basic univariate statistics are listed in Table 4-1 (water quality A). An initial review of the data indicated three important features.

(1) The data seemed to have strong anisotropy at about 150 counterclockwise degrees to the east-west baseline.

(2) The data required a natural log transformation so the distribution was approximated by a normal distribution.

(3) No trends were indicated during preliminary exploration, and ordinary kriging was tentatively selected as the appropriate technique.

c. Natural log transformations are routinely needed for concentration data that vary over several orders of magnitude, which is common in areas of contaminant plumes. The data were transformed to log space and fit acceptable criteria for normality. After transformation to log space, the techniques described in Chapter 4 were used to guide the following steps for variogram construction:

(1) An exponential model was used to fit a directional variogram at an angle of 150 counterclockwise degrees to the east-west baseline. The variogram had a nugget of 1.00 log concentration squared, a sill of 3.20 log concentration squared, and a range of 1,295 m [Figure 5-8a and Table 5-1 (water quality A)].

(2) An exponential model was also fit to a directional variogram at an angle of 240 counterclockwise degrees to the east-west baseline. The variogram had a nugget of 1.00 log concentration squared, a sill of 3.20 log concentration squared, and a range of 229 m [Figure 5-8b and Table 5-1 (water quality A)].

(3) Cross-validation was performed using the geometric anisotropy of the two variograms and the results [Figures 5-8c and 5-8d, and Table 5-1 (water quality A)] were acceptable.

d. The residuals are symmetrically distributed, (Figure 5-8d). However, the scatterplot (Figure 5-8c) indicates that small concentrations are overestimated and that large concentrations are underestimated. This discrepancy in the estimates does not indicate an error in the model, but rather, indicates a consequence of data that have a large nugget compared to the sill; in this example the nugget is approximately 30 percent of the sill. The large nugget decreases the predictive capacity of the model and increases the smoothing introduced by kriging.

e. The established variogram then was used, along with the measured locations, to produce ordinary kriging estimates for all points in a 40-by-20 grid using a grid spacing of about 91-by-91 m. For the kriging procedure, a search radius of about 1,524 m with maximum of 16 and a minimum of 8 locations was specified. Gray- scale maps of kriging estimates, back transformed to concentrations and in log space, as well as the kriging standard deviations in log space, are shown in Figures 5-9a, 5-9b, and 5-9c.

f. The back-transformation procedure was a simple exponentiation of the log space kriging estimates. Such a back-transformation does not use bias-correction factors to deal with moment bias and, consequently, the back-transformed values must be interpreted as a median value rather than a mean value. The simple back-transformation, however, is convenient and was performed, principally, to enhance visual interpretation of the kriging estimates. Univariate statistics for the log-space kriging estimates are listed in Table 5-2 (water quality A). The kriging results do have noticeable smoothing; however, they also indicate a plume emanating from an area just northwest of the center of the area and movement, as well as some dispersion, to the southeast; the estimates are a very good representation of the results from many other more elaborate studies.

g. An additional comment concerning log transformations is appropriate. To indicate the effect of the log transform on probabilities in

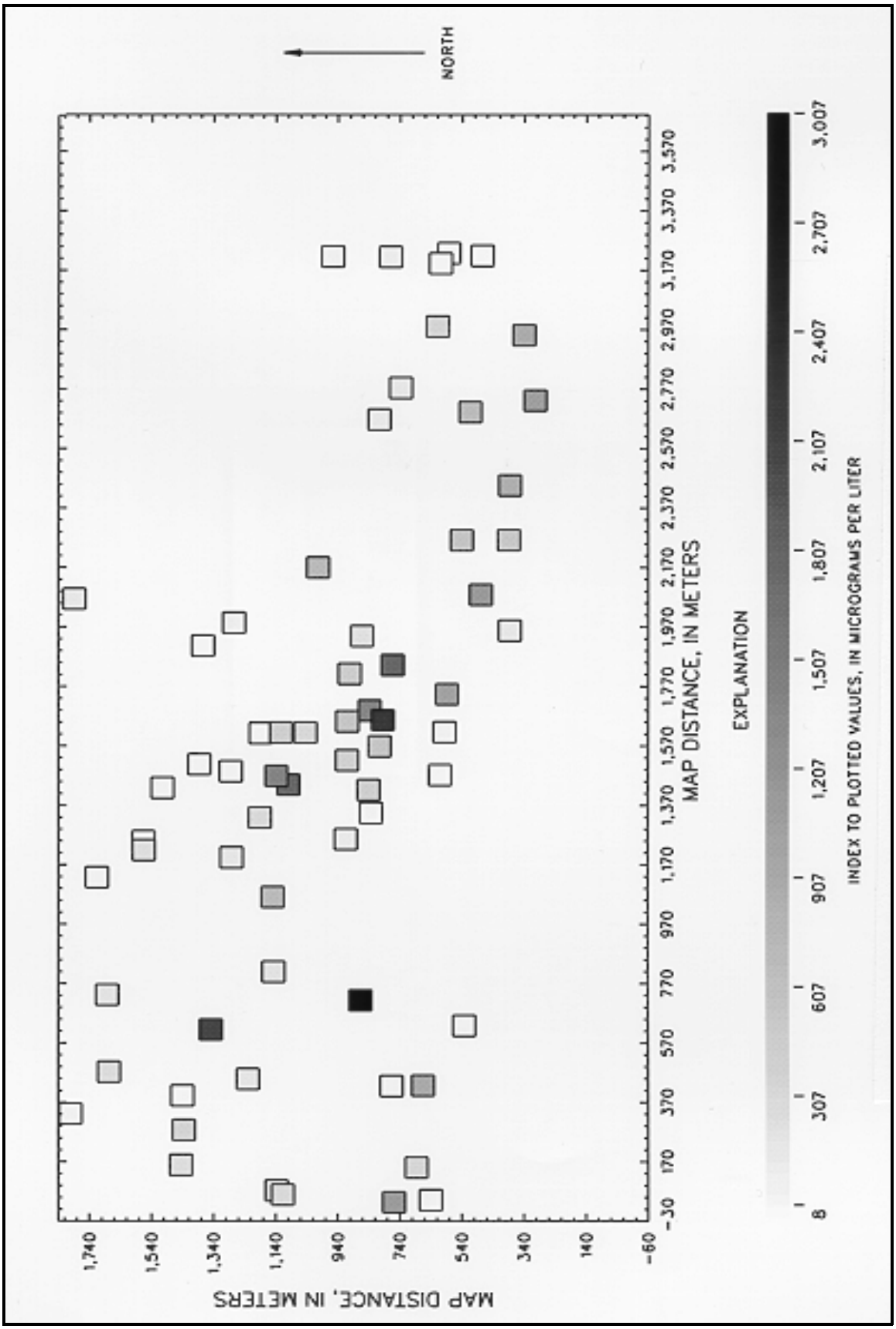

Figure 5-7. Measured data for water-quality examples

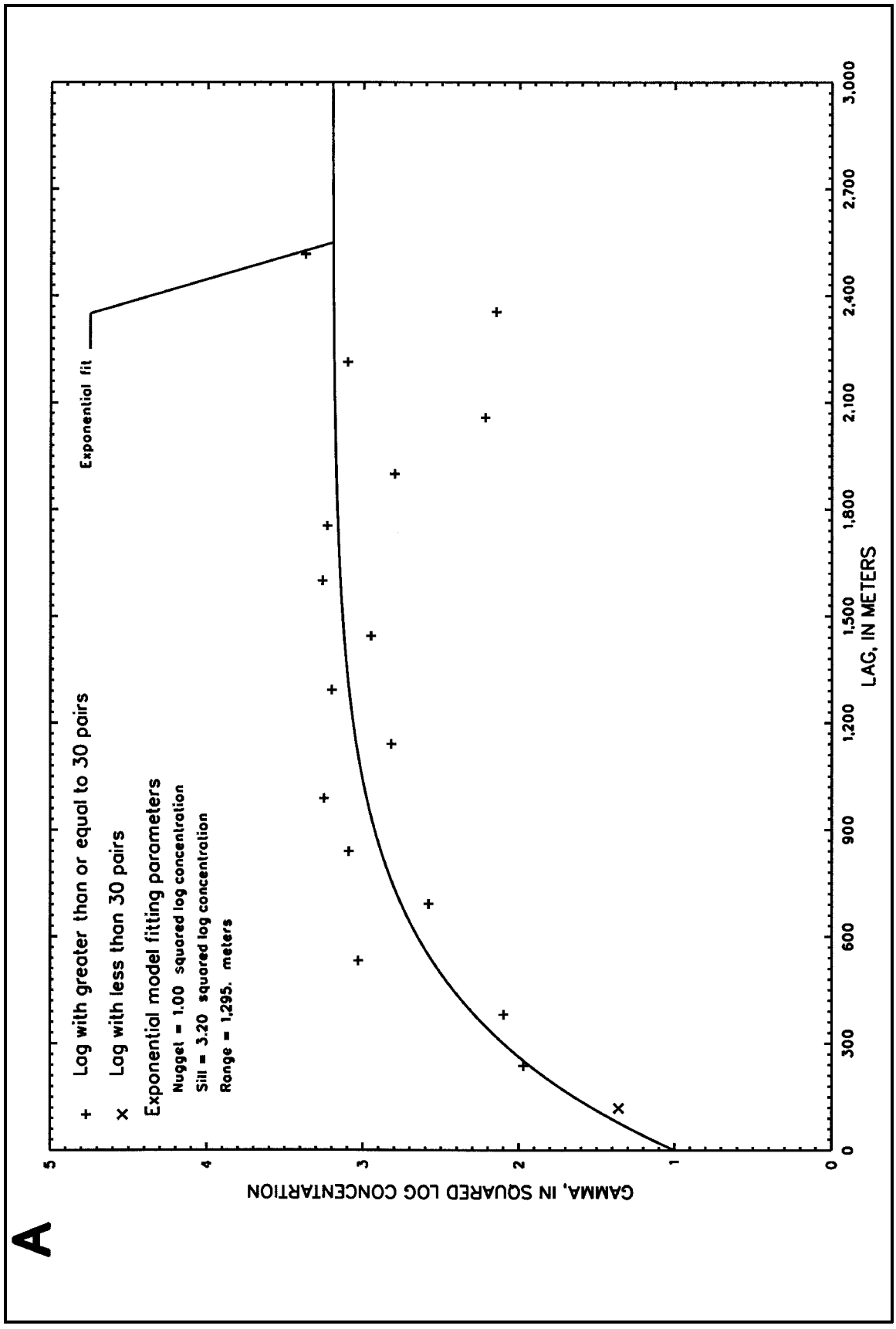

Figure 5-8. Directional variograms and variogram cross-validation plots for water-quality example--A, theoretical major-direction variogram (southeast); B, theoretical minor-direction variogram (northeast); C, cross-validation scatterplot; D, cross-validation probability plot (Sheet 1 of 4)

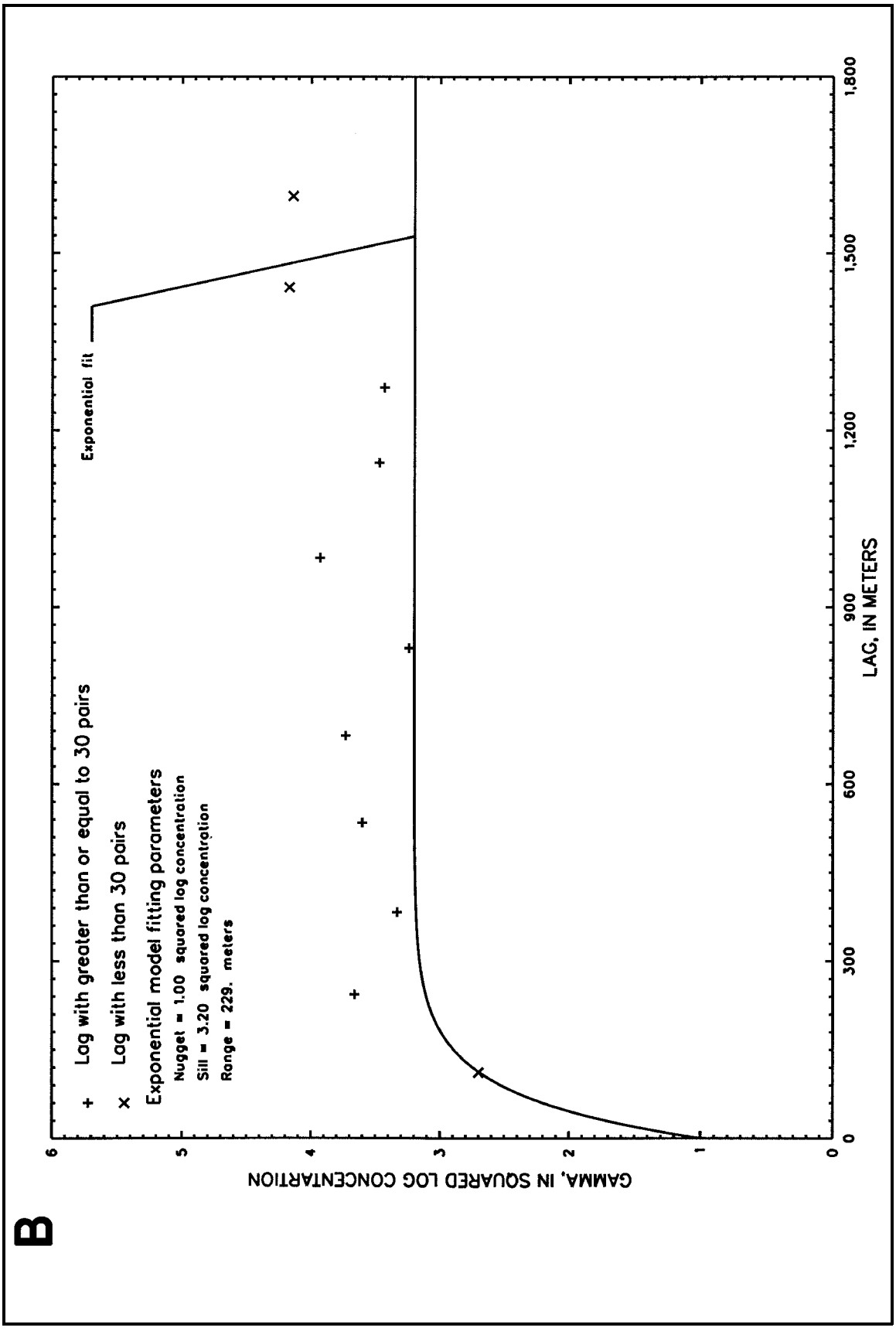

Figure 5-8. (Sheet 2 of 4)

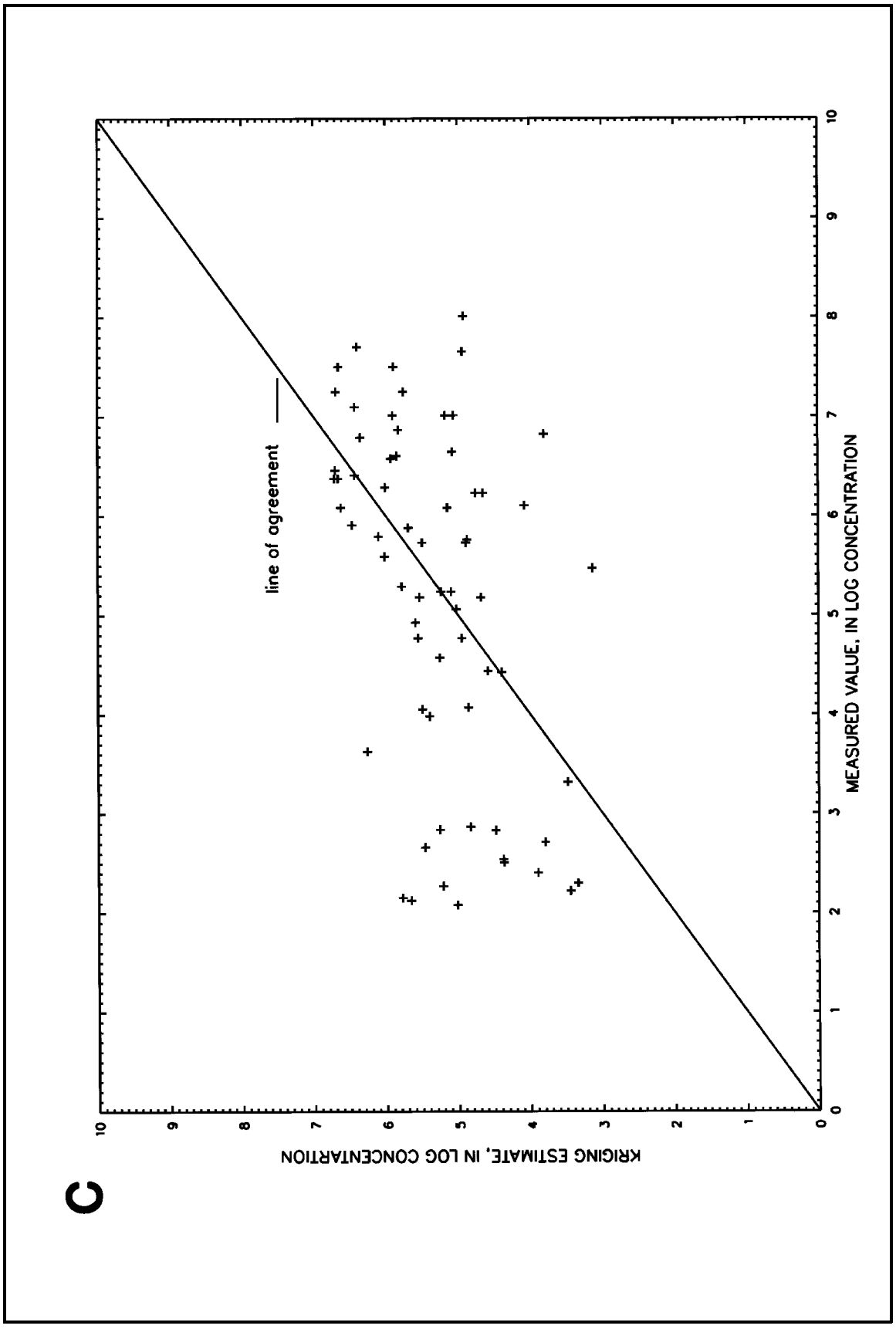

Figure 5-8. (Sheet 3 of 4)

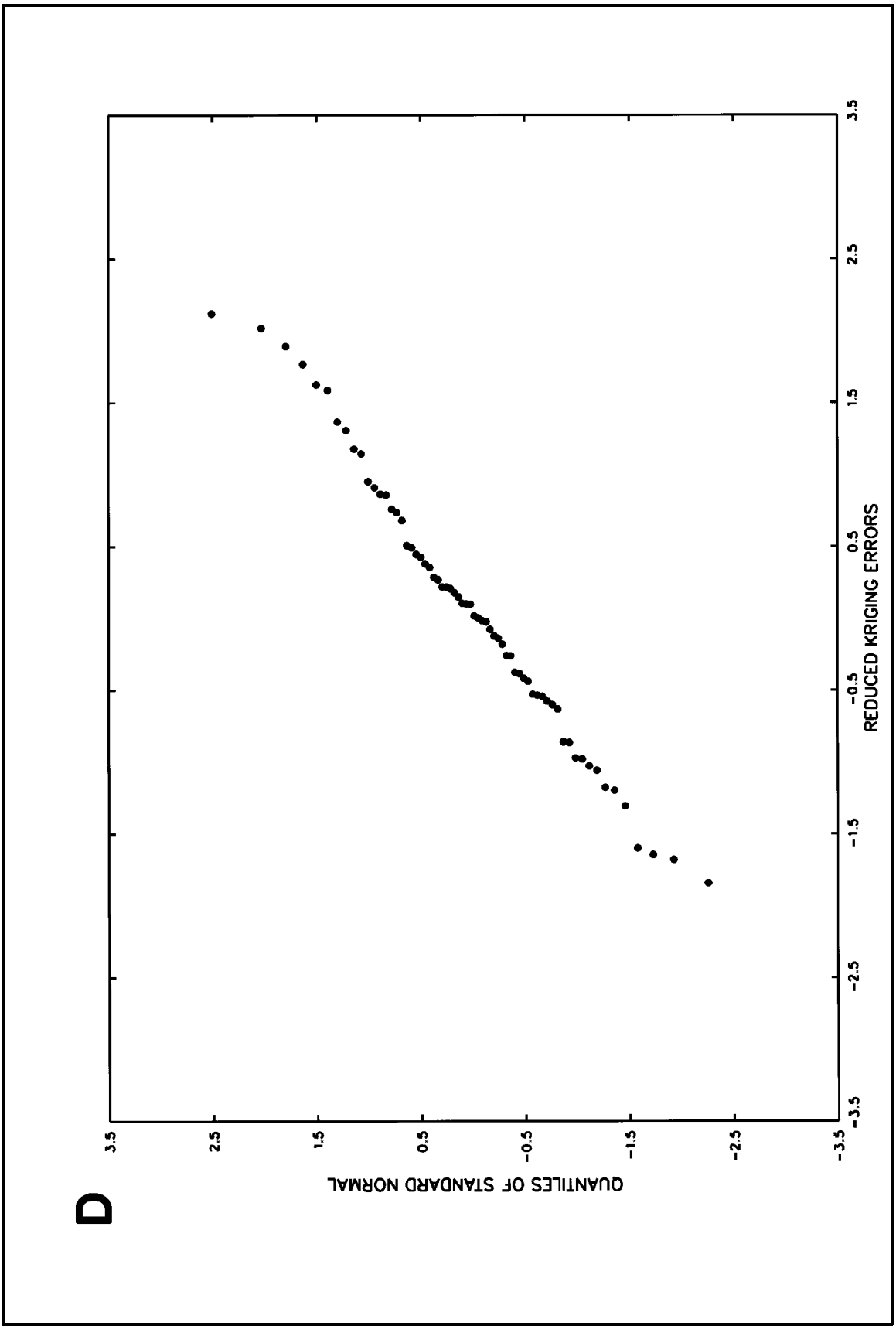

Figure 5-8. (Sheet 4 of 4)

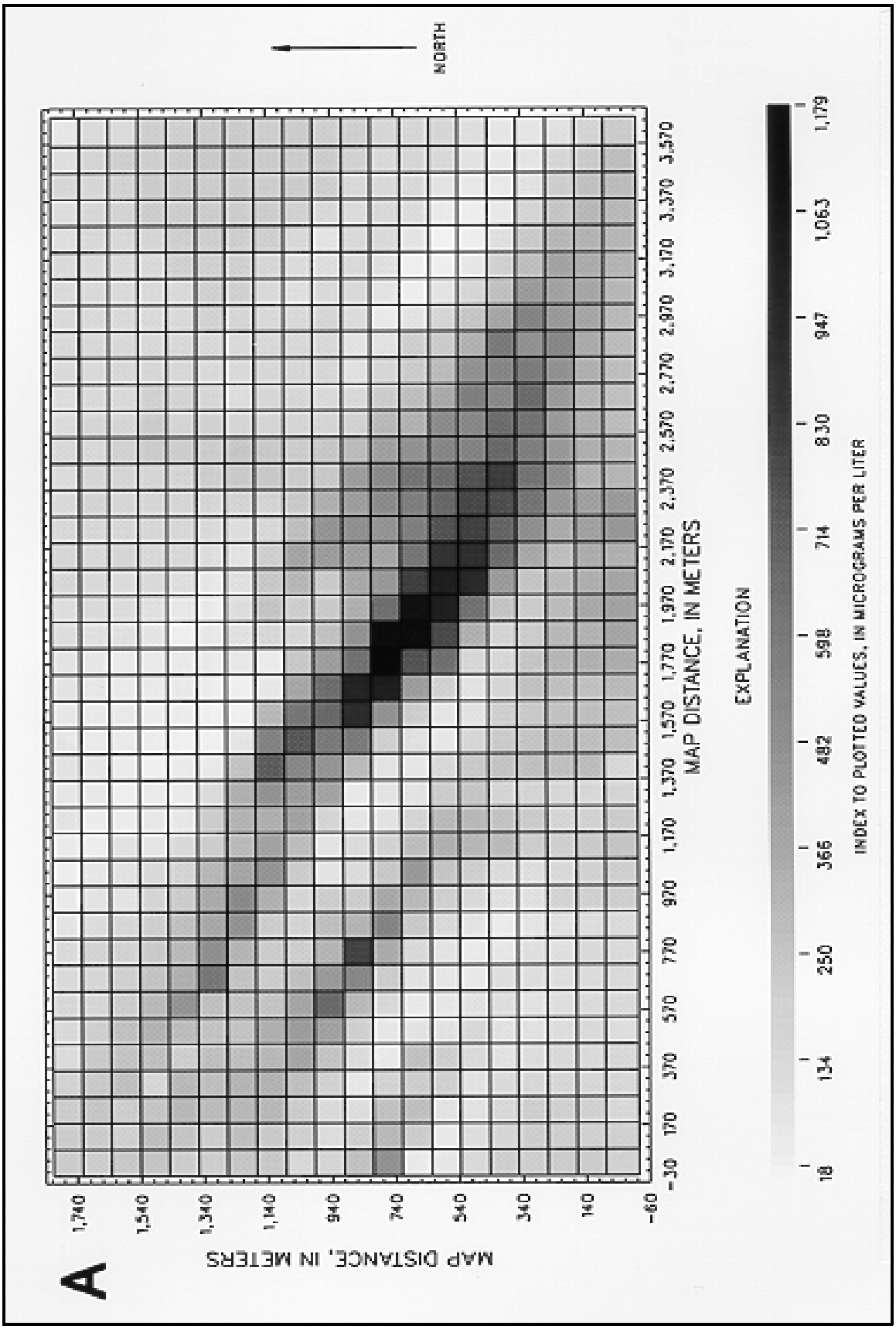

Figure 5-9. Kriging results for water-quality examples--A, kriging estimates back-transformed; B, kriging estimates in lot space; C, kriging standard deviations in lot space; D, 95-percent confidence level of kriging estimates back-transformed (Sheet 1 of 4)

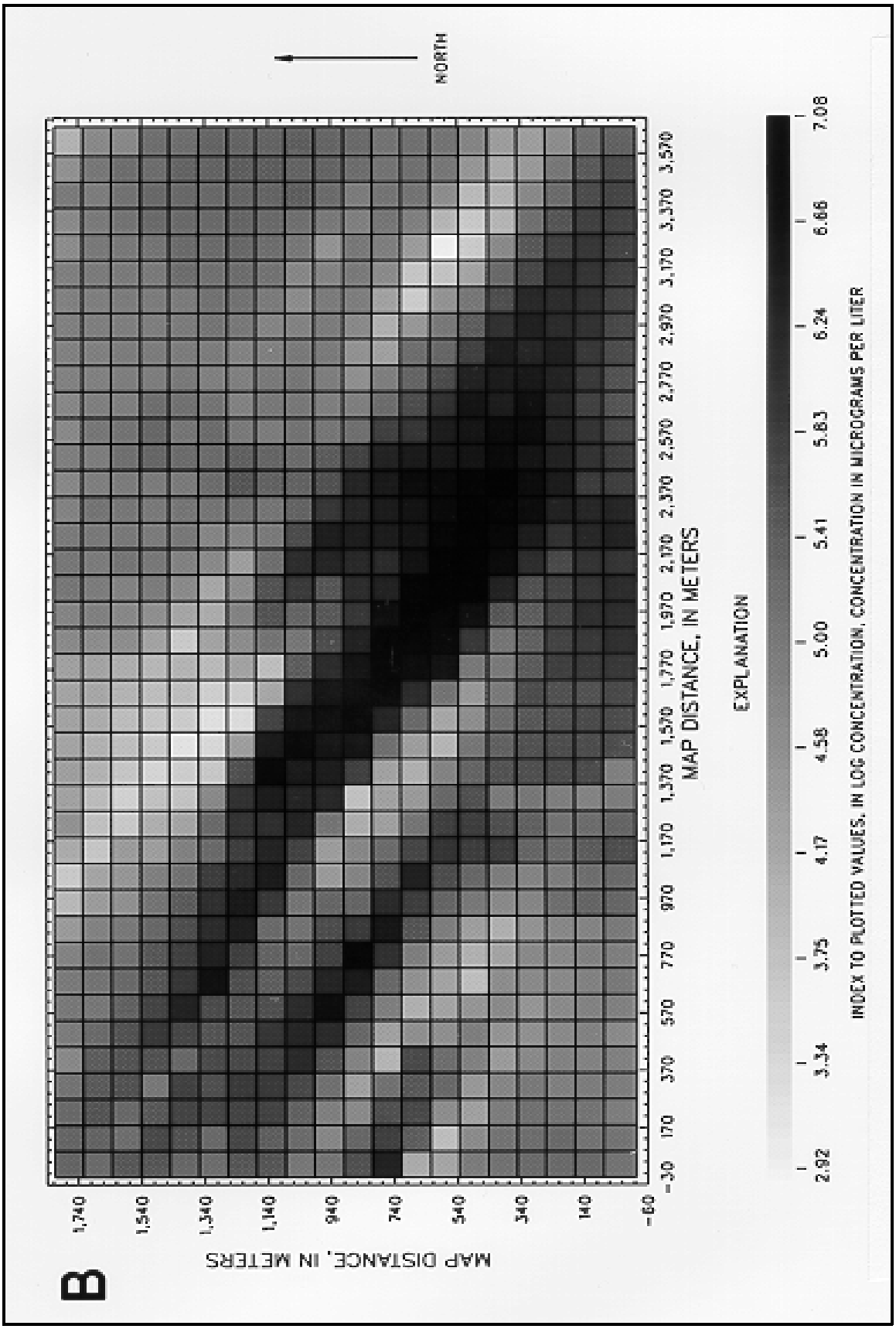

Figure 5-9. (Sheet 2 of 4)

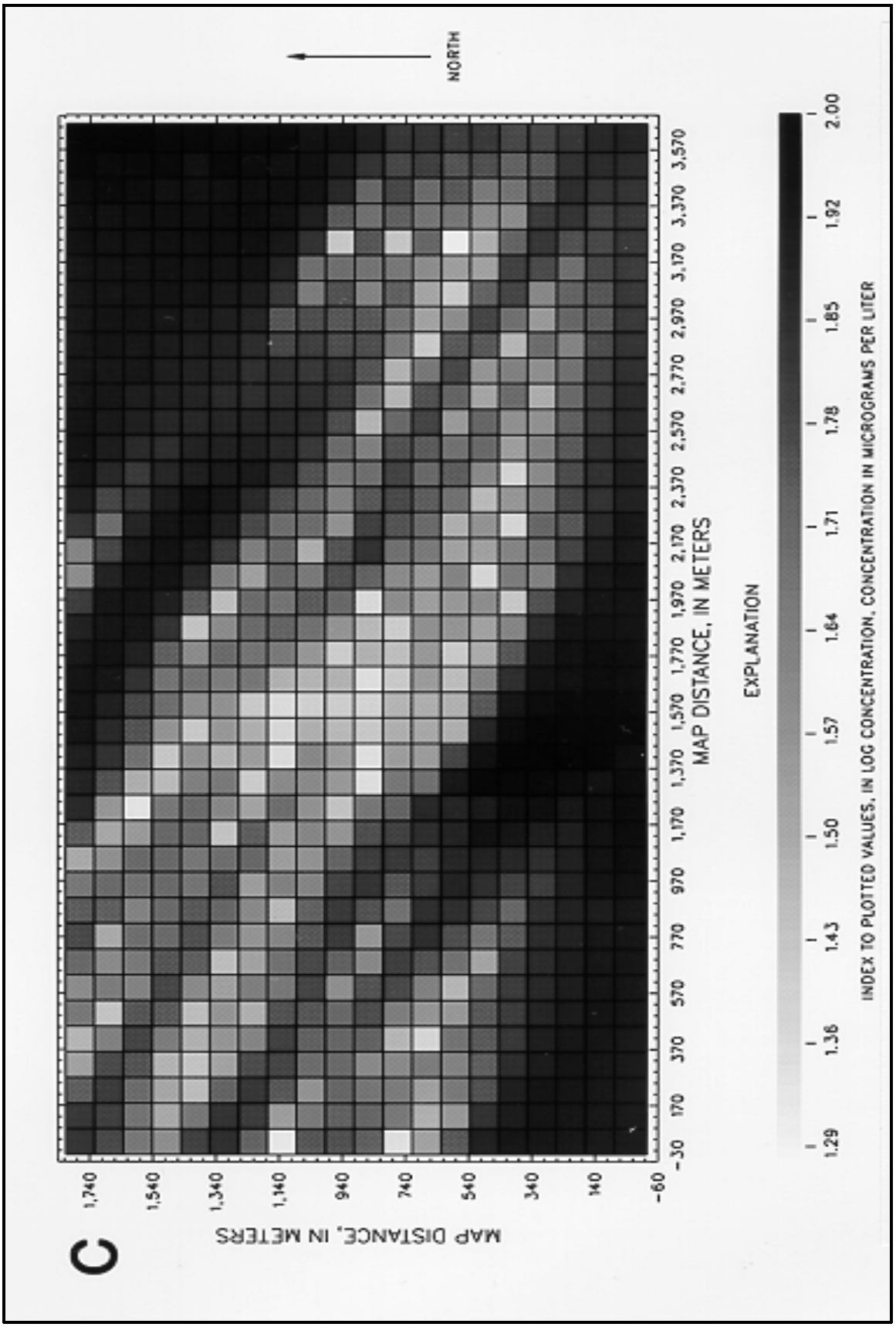

Figure 5-9. (Sheet 3 of 4)

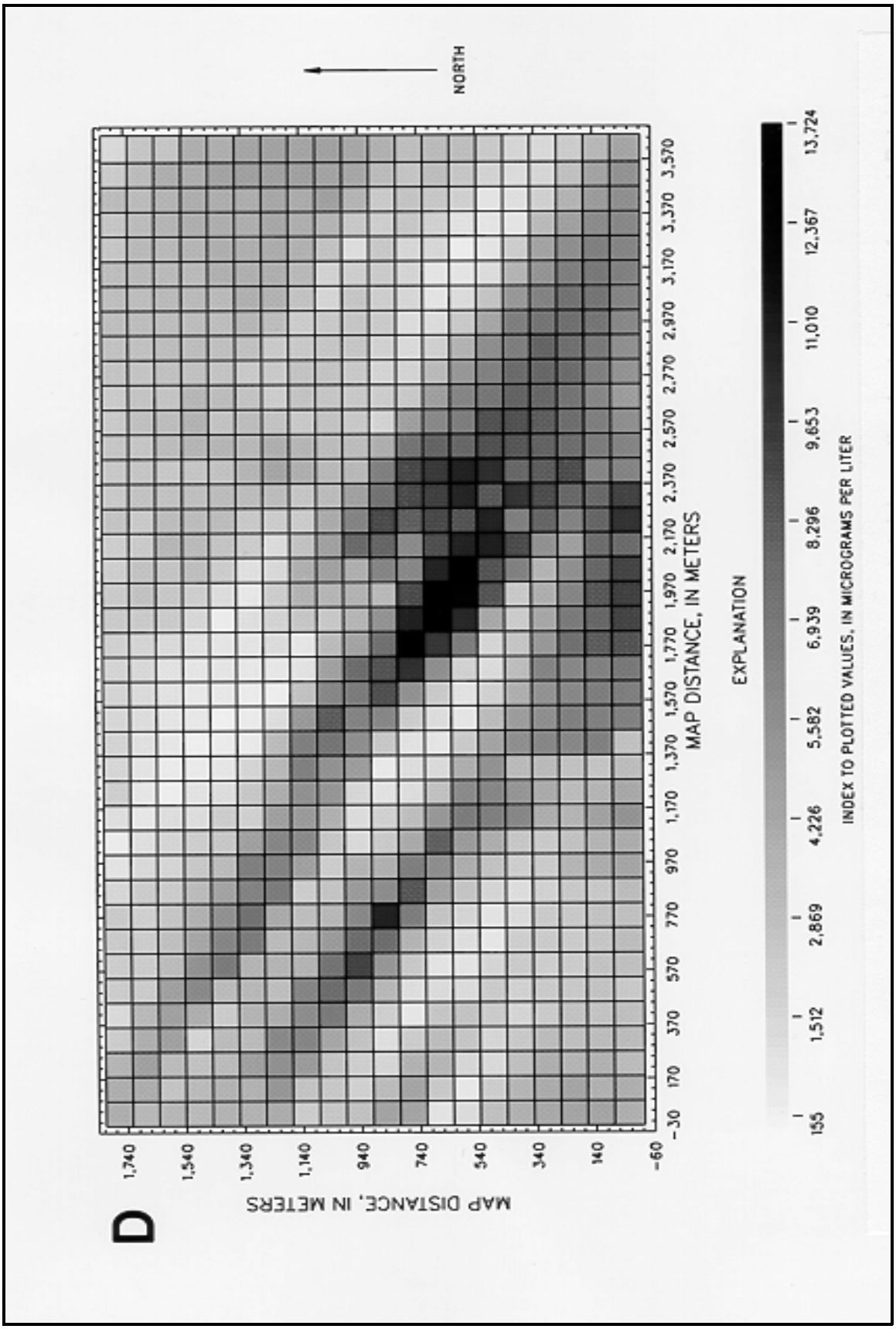

Figure 5-9. (Sheet 4 of 4)

converting, or back-transforming, kriging estimates, the kriging estimates and the kriging standard deviations, in log space, were used to estimate the one-sided 95th percentile at each kriging-estimate location according to the formula:

$$\hat{C}_{0.95} = \exp\left[\hat{Z}(\underline{x}_0) + 1.645\sigma_K(\underline{x}_0)\right] \quad (5\text{-}1)$$

where $(\hat{Z}\ \underline{x}_0)$ (is the kriging estimate at location $\underline{x}_0$, in log space, and $\sigma_k(\underline{x}_0)$ is the corresponding kriging standard deviation in log space. The resulting map is shown in Figure 5-9d. Such a map can be used to indicate areas where the true concentration has only a 5-percent chance of exceeding the value shown.

h. To perform indicator kriging, the indicator transformation, as described in Chapter 2, was applied. An indicator cutoff equal to the median value of 270 for the untransformed measured data was selected. The model for indicator kriging estimates the probability that the concentration would be less than the indicator cutoff. The techniques described in Chapter 4 were used to guide the following steps in variogram construction:

(1) No trends were indicated during preliminary exploration, and ordinary kriging was tentatively selected as the appropriate technique.

(2) A spherical model was used to fit an anisotropic variogram at an angle of 150 deg counterclockwise to the east-west baseline. The variogram had a nugget of 0.05 indicator units squared, a sill of 0.25 indicator units squared, and a range of 610 m [Figure 5-10a and Table 5-1 (water quality B)].

(3) A spherical model also was fit to an anisotropic variogram at an angle of 240 deg counterclockwise to the east-west baseline. The variogram had a nugget of 0.05 indicator units squared, a sill of 0.25 indicator units squared, and a range of 213 m [Figure 5-10b and Table 5-1 (water quality B].

i. The established variogram, along with the indicator transform of the measured data, was used to produce ordinary kriging estimates for the same grid and search criteria as the first water-quality example. A gray-scale map of the kriging estimates is shown in Figure 5-11. The kriging indicator map provides a gridded estimate for the probability of contaminant values being less than the indicator cutoff, which is a concentration of 270 in this example.

j. The cutoff value selected for the preceding indicator kriging example is probably higher than many investigators involved in HTRW site investigations would like to use. In this case the number of measurements [66 in Table 4-1 (water quality B)] used in this example, which is probably a high number of measurements for typical HTRW site investigations, would not permit construction of an indicator variogram for indicator values much lower than the median. An alternative to this problem would be to assume that the log-transformed kriging model developed in the first water-quality example is correct and to rely on the kriging estimates from that model to determine areas greater than or less than some indicator value. The same estimates also could be used to compute the probability that the concentration was less than some arbitrarily selected value.

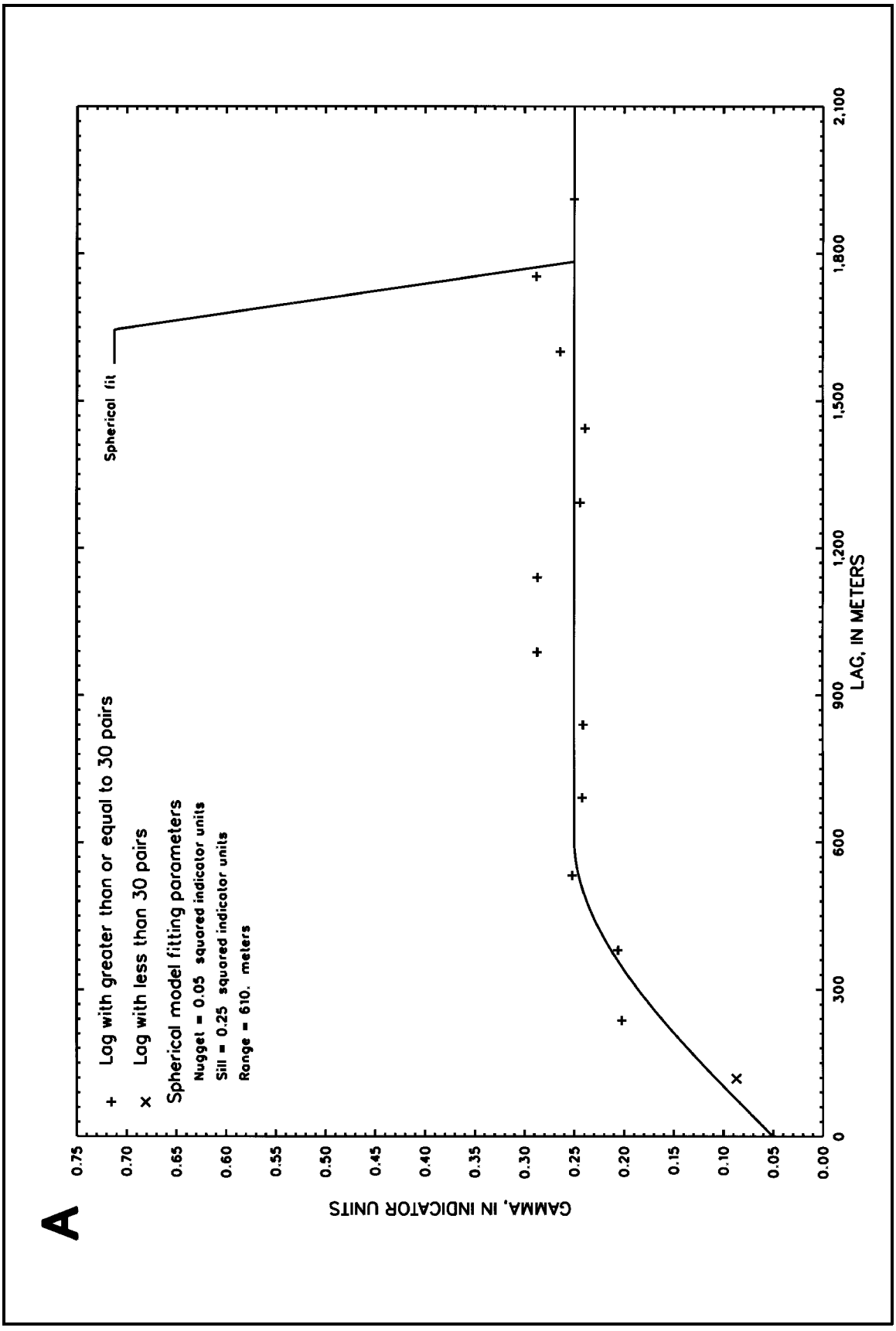

Figure 5-10. Directional variogram plots for indicator kriging water-quality example--A, theoretical major-direction variogram, and B, theoretical minor-direction variogram (Continued)

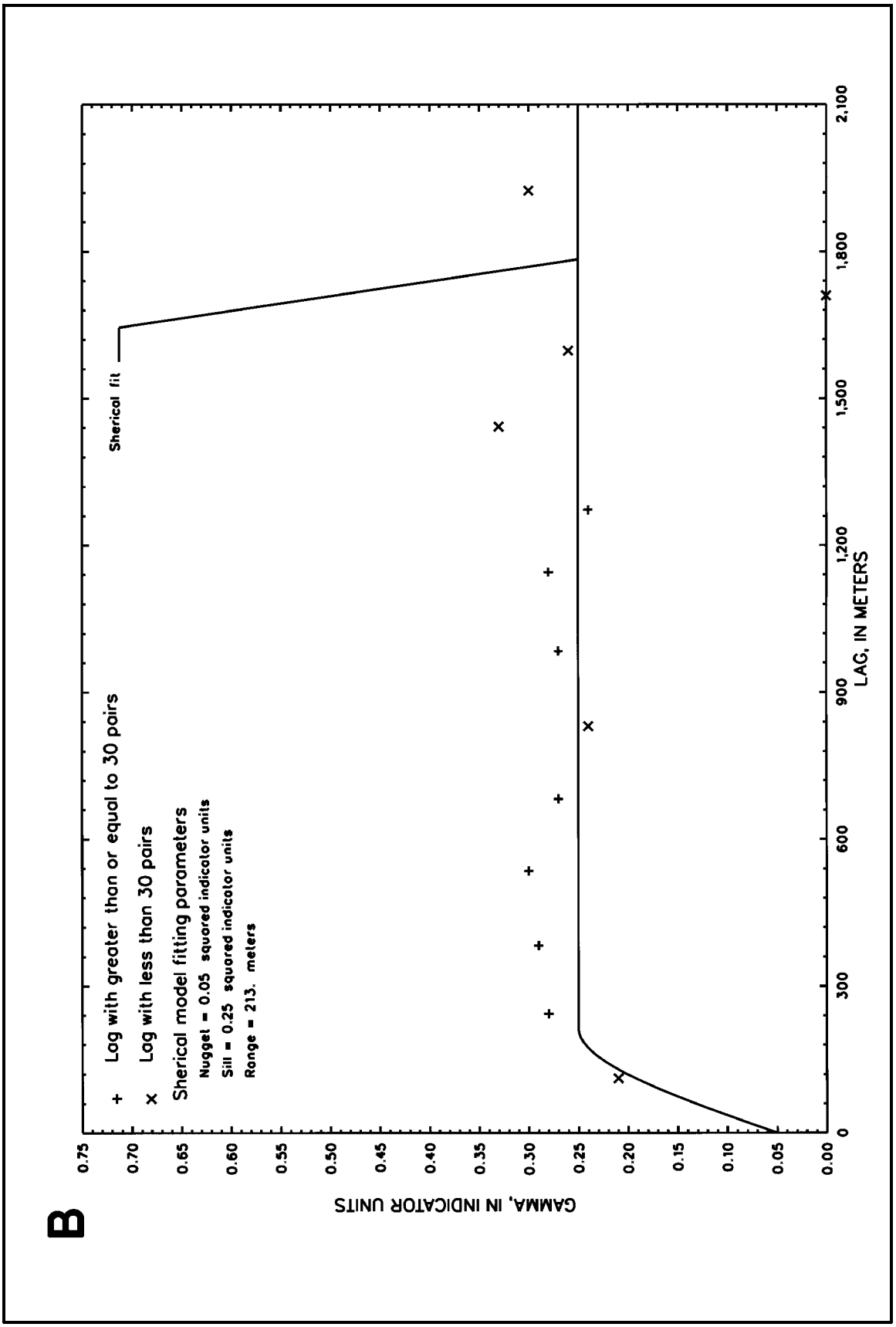

Figure 5-10. (Concluded)

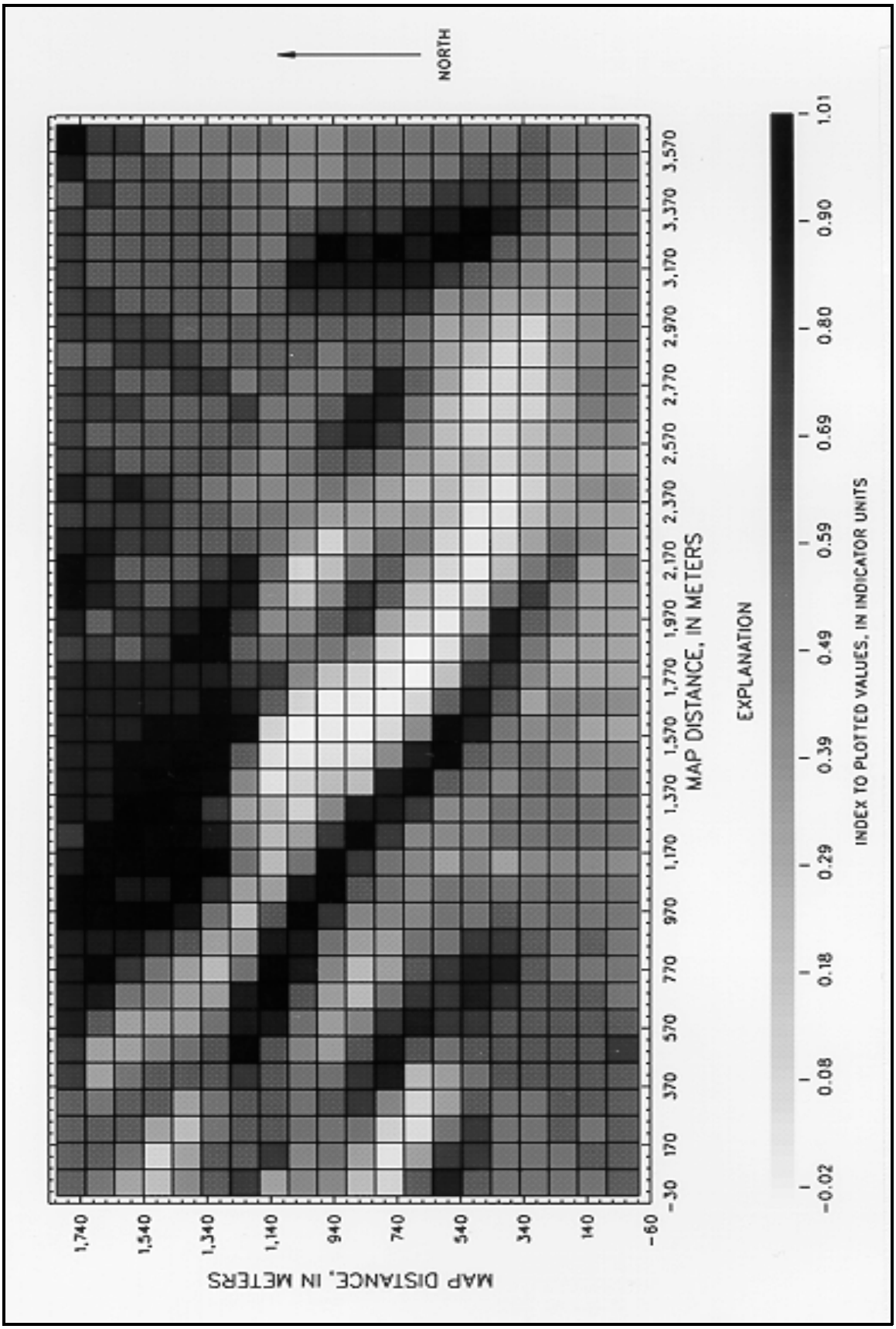

Figure 5-11. Indicator kriging results for water-quality example